

Space Charge Induced Beam Emittance Growth and Halo Formation

Space charge effect resulted in beam emittance growth are typically can be divided by two classes:

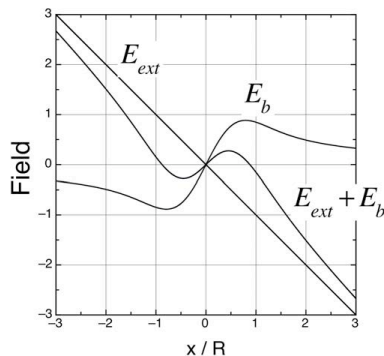
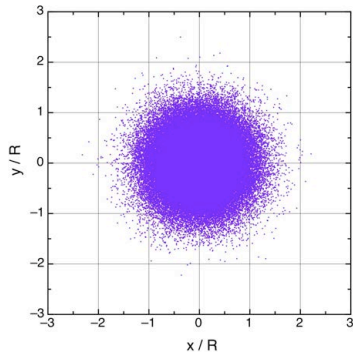
(i) single particle dynamics in collective space charge field of “pseudo” multipoles (incoherent space charge effects):

- Space charge aberrations
- “Free Energy” effect
- Excitation of nonlinear resonances
- Particle-core interaction

(ii) instabilities and resonances of beam distribution (coherent space charge effects).

Effect of Space Charge Aberration on Beam Emittance

Space charge density and space charge field of the beam with Gaussian distribution are given by



$$\rho(r_o) = \frac{2I}{\pi R_o^2 \beta c} \exp(-2 \frac{r_o^2}{R_o^2})$$

$$E_b = \frac{I}{2\pi \epsilon_0 \beta c} \frac{1}{r_o} [1 - \exp(-2 \frac{r_o^2}{R_o^2})]$$

Nonlinear function in space charge field is expanded as

$$f(r_o) = 1 - \exp(-2 \frac{r_o^2}{R_o^2}) \approx 2 \frac{r_o^2}{R_o^2} - 2 \frac{r_o^4}{R_o^4} + \dots$$

At the initial stage of beam emittance growth we can assume, that particle radius is unchanged, while the slope of the trajectory is changed. It gives us the nonlinear transformation:

$$r = r_o$$

$$r' = r_o + \frac{2zP^2}{R_o^2} r_o - \frac{2zP^2}{R_o^4} r_o^3$$

where $P^2 = \frac{2I}{I_c \beta^3 \gamma^3}$ is the generalized perveance, $I_c = 4\pi\epsilon_0 mc^3 / q$ is the characteristic beam current.

Effect of Space Charge Aberration on Beam Emittance

Parameter ν , which determines effect of spherical aberration on beam emittance is

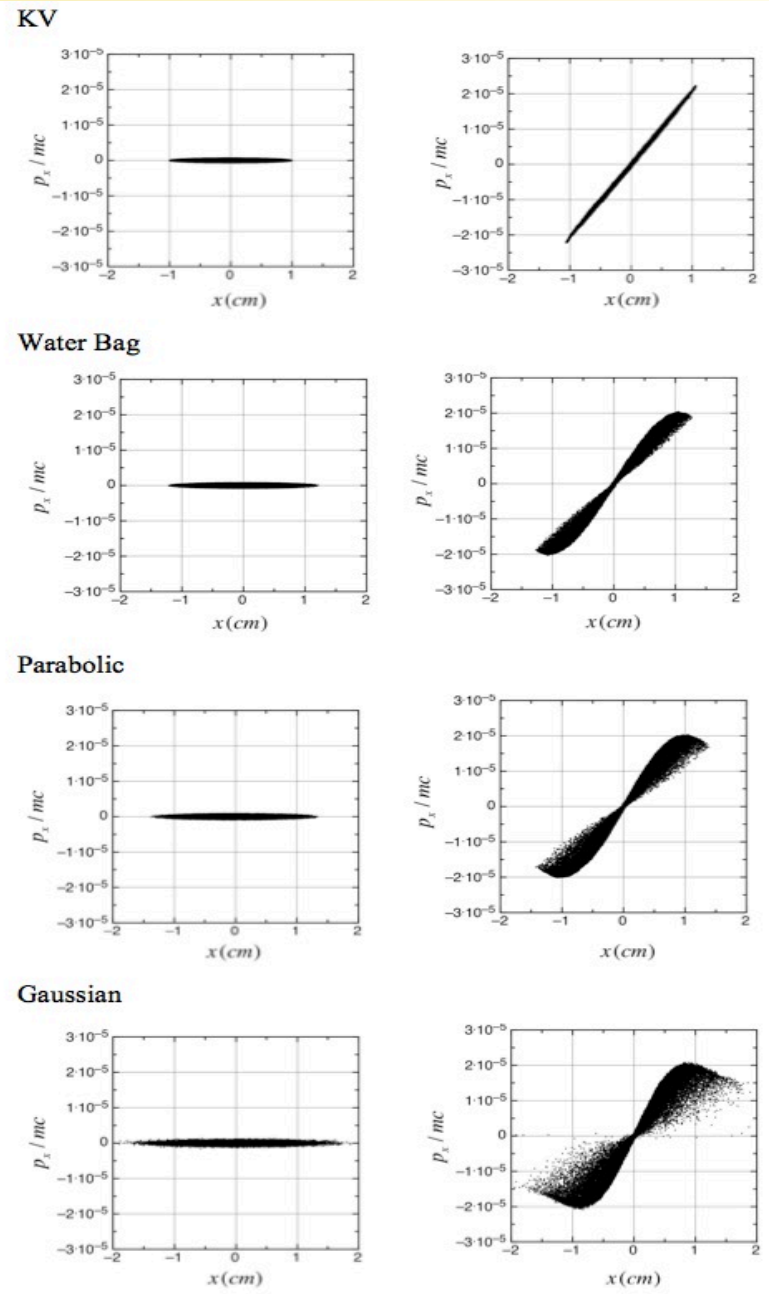
$$\frac{C_\alpha R_o^4}{f\Theta} = \frac{4}{\beta^3 \gamma^3} \frac{I}{I_c} \frac{z}{\Theta}$$

Therefore, space charge induced beam emittance growth in free space is:

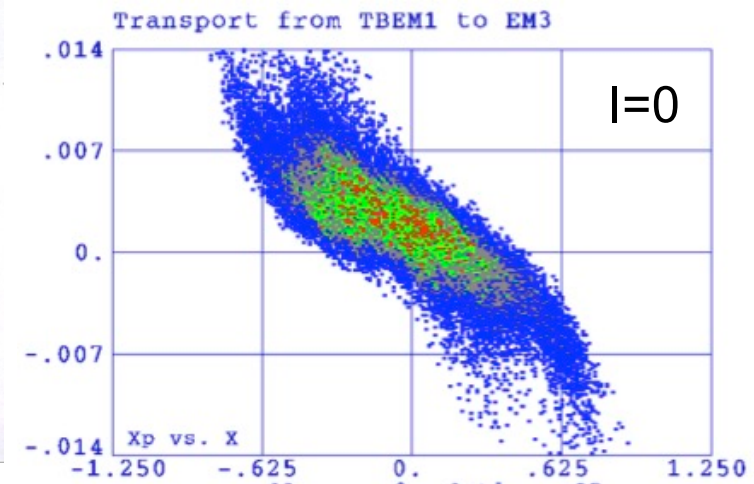
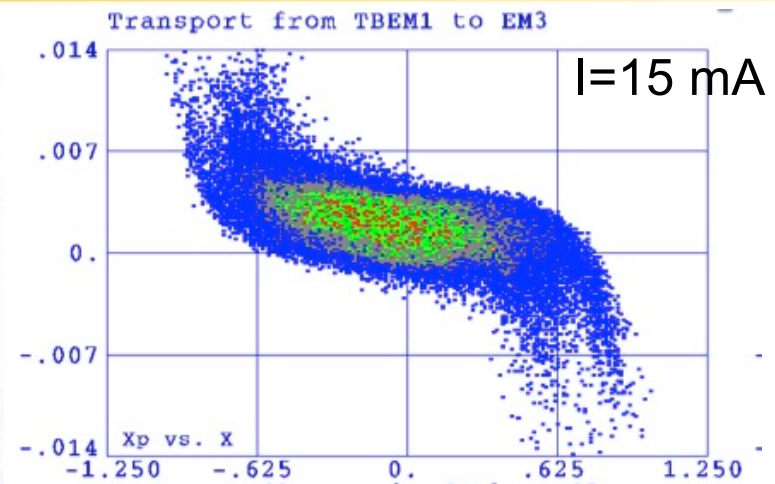
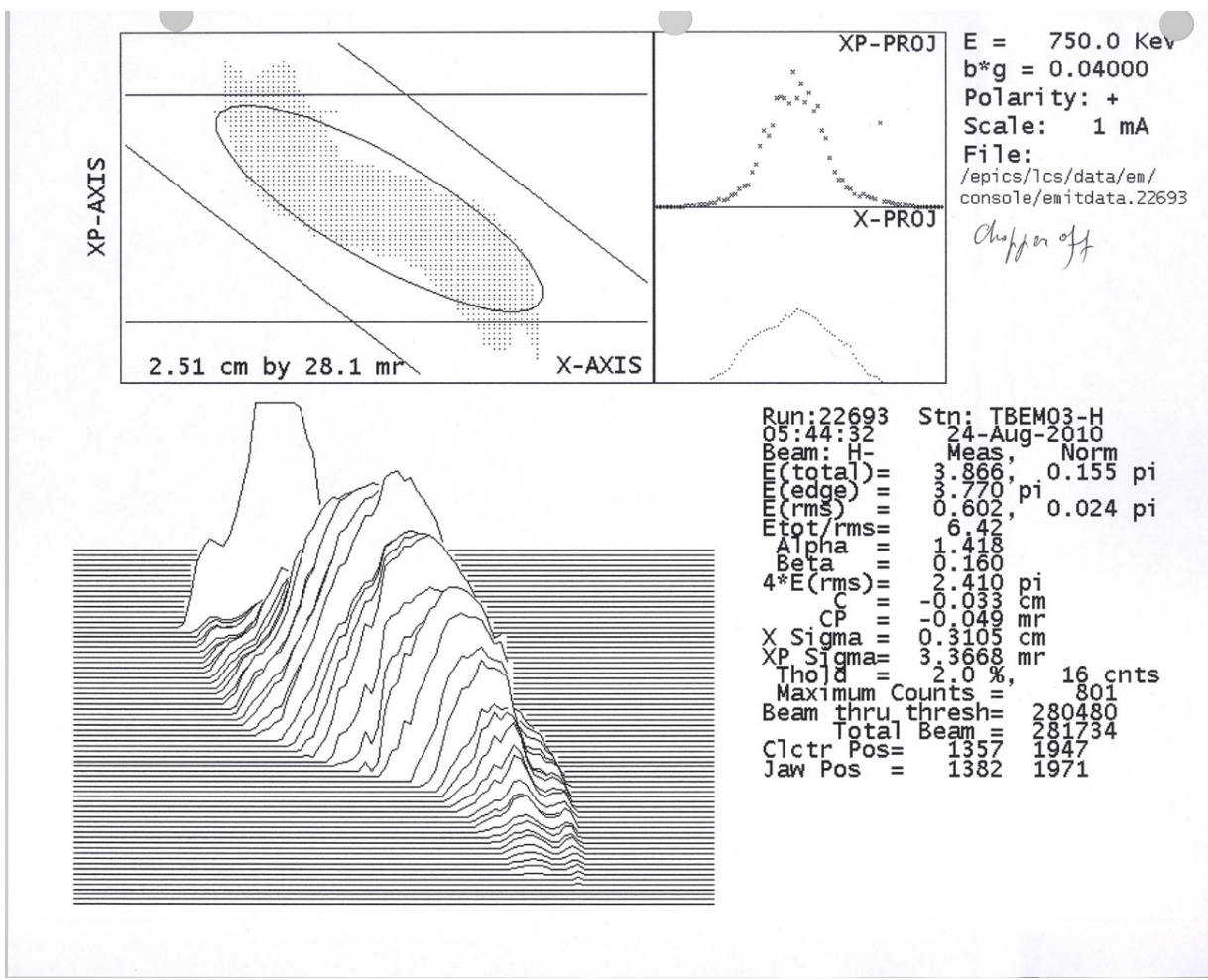
$$\frac{\Theta_{eff}}{\Theta} = \sqrt{1 + \bar{K} \left(\frac{I}{I_c \beta^3 \gamma^3} \frac{z}{\Theta} \right)^2}$$

Parameter \bar{K} was determined numerically for different distributions. Results are summarized in Table. As follows from above equation, initial emittance growth does not depend on initial beam radius.

Distribution	Coeff.
	\bar{K}
KV	0
Water Bag	0.094
Parabolic	0.187
Gaussian	0.55



Experimental Observation of Effect of Nonlinear Space Charge Forces on Beam Emittance



(Y.B. et al, Proc. of PAC2011, p. 64)

Effect of Elliptical Cross Section on Beam Emittance Growth

Suppose that the density is parabolic, given by

$$n(x, y) = \frac{2N_1}{\pi ab} \left[1 - \frac{x^2}{a^2} - \frac{y^2}{b^2} \right],$$

within the boundary of the ellipse defined by

$$\frac{x^2}{a^2} + \frac{y^2}{b^2} = 1.$$

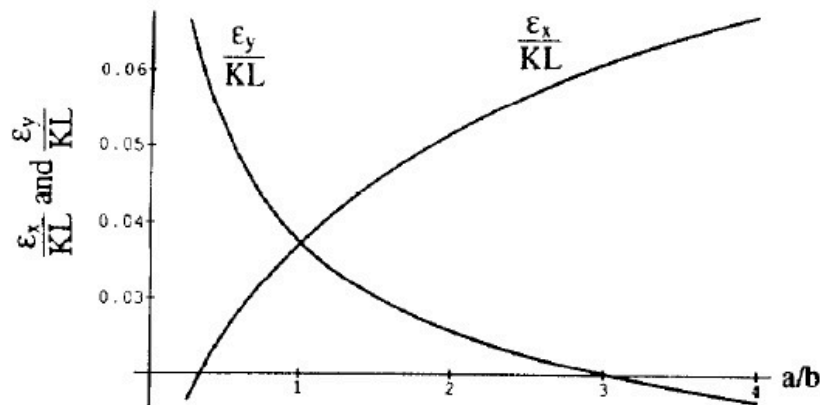


Figure 4. Final rms emittance values versus ellipse-aspect ratio a/b for a beam with parabolic density.

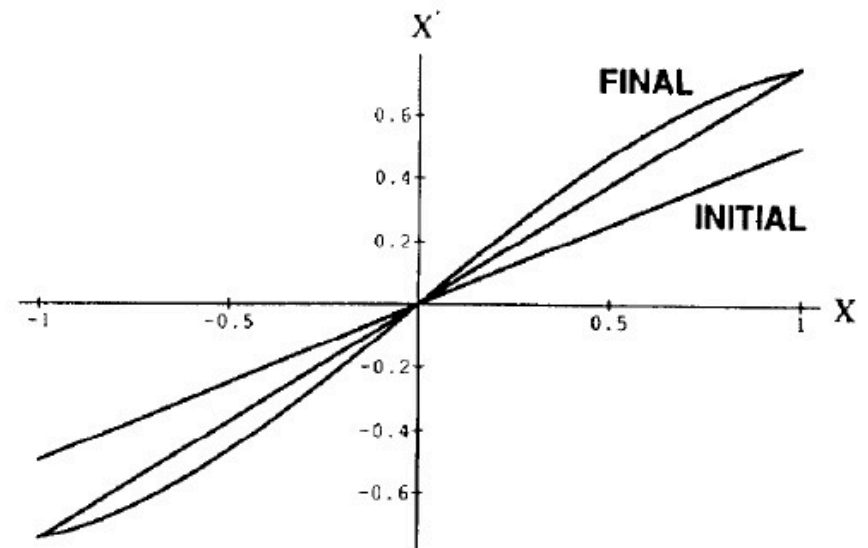


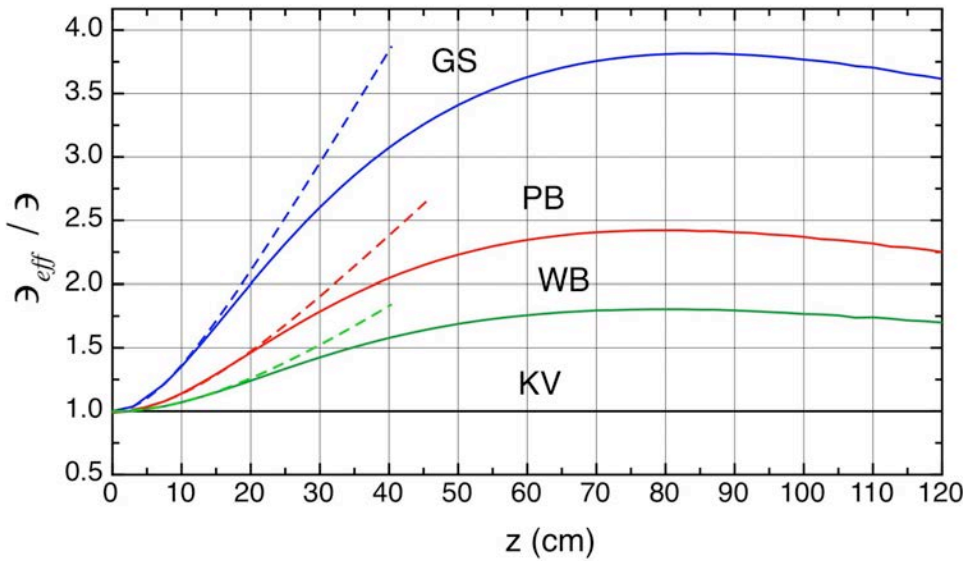
Figure 3. Effect of space charge from a parabolic density on an initial zero-emittance beam. The initial and final phase-space distributions are shown.

$$\epsilon_x = KL \frac{a}{b} \sqrt{\frac{1}{432} \frac{\left(\frac{2a}{b} + 1\right)^2}{\left\{1 + \frac{a}{b}\right\}^4} + \frac{7}{720} \frac{1}{\left\{1 + \frac{a}{b}\right\}^4} - \frac{1}{360} \frac{\left(\frac{2a}{b} + 1\right)}{\left\{1 + \frac{a}{b}\right\}^4}}.$$

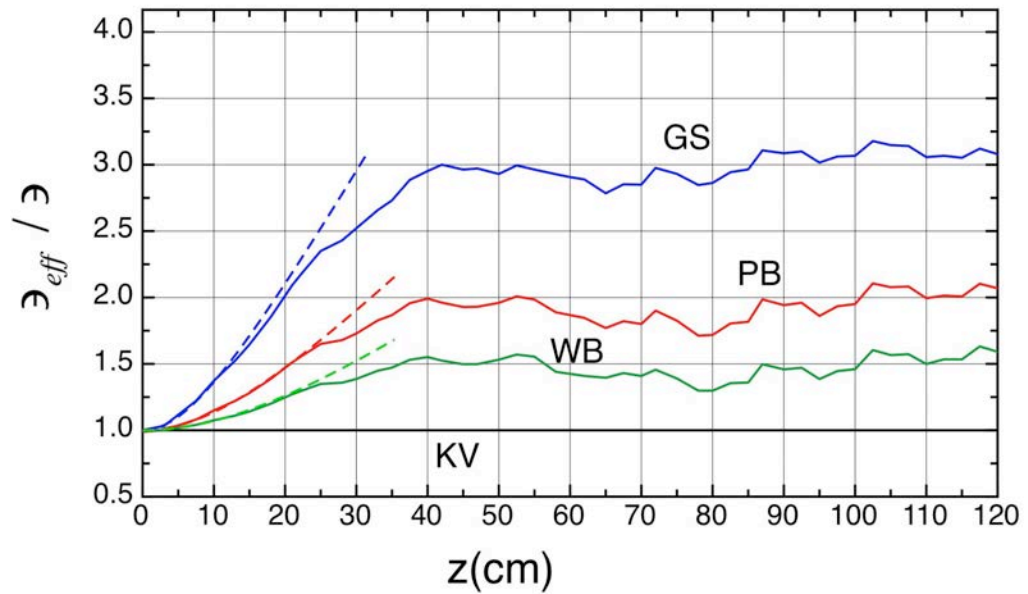
(T.Wangler, P.Lapostolle, A.Lombardi, PAC 1993, p.3606)

Space Charge Induced Beam Emittance Growth

Drift



FODO Channel



Emittance growth of a 50 keV proton beam with current $I = 20$ mA and unnormalized emittance $4.64 \pi \text{ cm mrad}$ in drift space and in FODO focusing channel for different beam distributions: (solid) simulations, (dotted) aberration approximation.

Space Charge Induced Beam Emittance Growth in a Focusing Channel (“Free Energy” Effect)

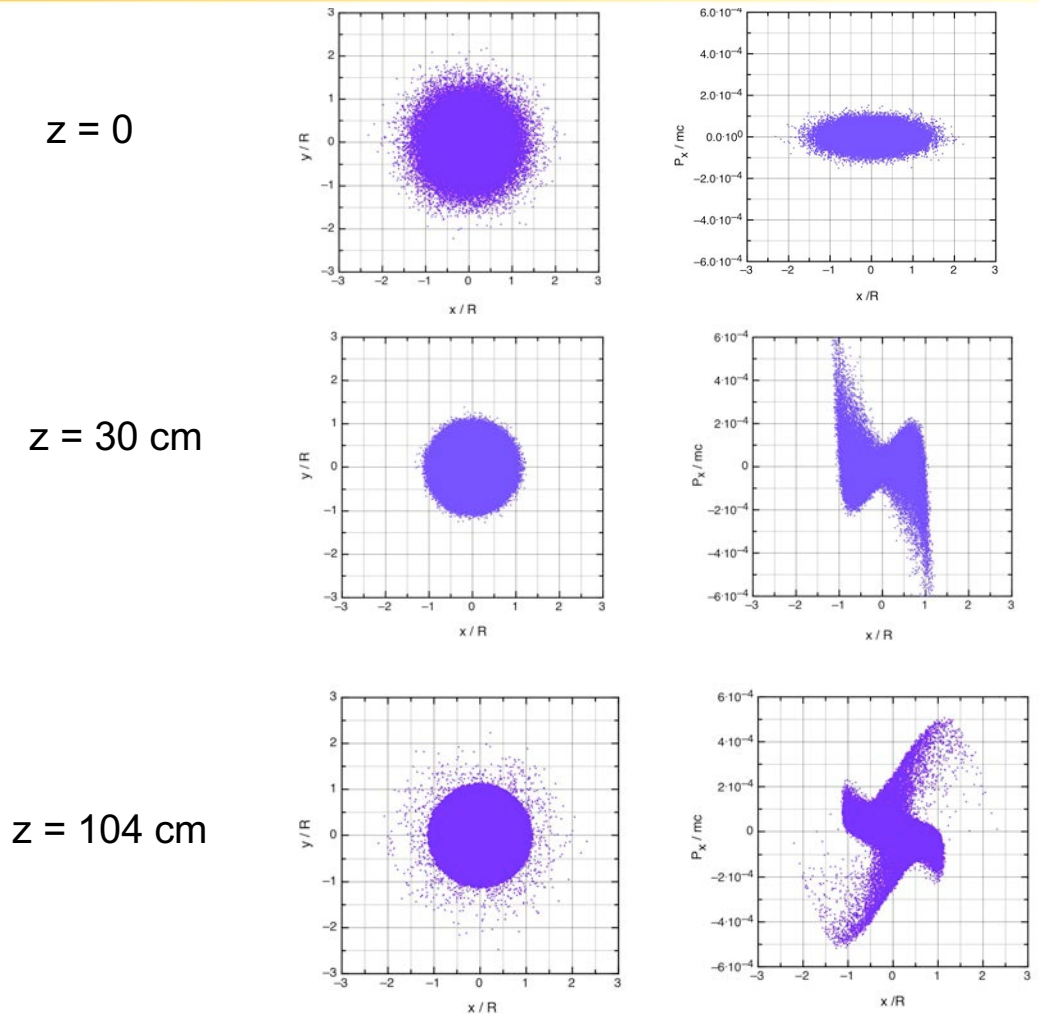


Fig. 3.7. Injection of 135 keV, 100 mA, $0.07 \pi \text{ cm mrad}$ proton beam with Gaussian distribution in a focusing channel with linear field. It results in

- (a) beam uniforming
- (b) beam emittance growth
- (c) halo formation.

Application of Poynting's Theorem

Conservation of energy for electromagnetic field (Umov-Poynting's theorem)

$$\oint_S [\vec{E}, \vec{H}] d\vec{S} = - \frac{d}{dt} \int_V \left(\frac{\mu_0 H^2}{2} + \frac{\epsilon_0 E^2}{2} \right) dV - \int_V \vec{j} \cdot \vec{E} dV$$

Expression on the left side is an integral of Poynting's vector $\vec{\Pi} = [\vec{E}, \vec{H}]$ over surface S surrounding volume V and is equal to the power of electromagnetic irradiation, or energy of electromagnetic field coming through the surface S per second. Because beam is propagating in conducting tube, no energy is transferred through it. The first integral in right side of Poynting theorem is a change of energy of electromagnetic field per second:

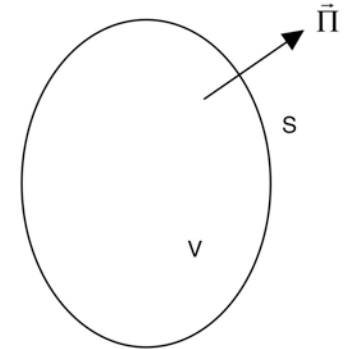
$$\frac{d}{dt} \int_V \left(\frac{\mu_0 H^2}{2} + \frac{\epsilon_0 E^2}{2} \right) dV = \frac{dW}{dt}$$

Second term in right side of Poynting theorem is a change of kinetic energy of the beam per second:

$$\int_V \vec{j} \cdot \vec{E} dV = \frac{d}{dt} \sum_{i=1}^N W_{kin}$$

For non-relativistic case (no magnetic field):

$$\frac{d}{dt} \left(\frac{\epsilon_0}{2} \int E^2 dV + \sum_{i=1}^N W_{kin} \right) = 0$$



Emittance Growth due to Charge Redistribution

where E is the total electrostatic field in the structure, and W_{kin} is the kinetic energy of particle:

$$W_{kin} = mc^2 \sqrt{1 + \frac{p_x^2 + p_y^2 + p_z^2}{(mc)^2}} \approx mc^2(\gamma - 1) + \frac{p_x^2 + p_y^2}{2m\gamma} \quad (3.62)$$

and summation is performed over all particles of the beam. Below consider only transverse particle motion and kinetic energy, associated with this motion. According to definition of rms beam values, kinetic energy of particles is:

$$\sum_{i=1}^N W_{kin} = \frac{N}{2m\gamma} [\langle p_x^2 \rangle + \langle p_y^2 \rangle] \quad (3.63)$$

where rms value of transverse momentum is

$$\langle p_x^2 \rangle = \left(\frac{mc\epsilon}{2R} \right)^2 \quad (3.64)$$

In a round beam rms values in both transverse directions are the same, $\langle p_x^2 \rangle = \langle p_y^2 \rangle$, therefore

$$\sum_{i=1}^N W_{kin} = N \frac{mc^2}{\gamma} \left(\frac{\epsilon}{2R} \right)^2 \quad (3.65)$$

Emittance Growth due to Charge Redistribution (cont.)

Finally, equation for conservation of total energy can be rewritten for matched beam ($R_f \approx R_o$) as

$$\frac{\epsilon_f}{\epsilon_i} = \sqrt{1 + (\frac{\mu_o^2}{\mu^2} - 1) (\frac{W_i - W_f}{W_o})}$$

where initial, W_i , and final, W_f , energy stored in electrostatic field are

$$W_i = \frac{\epsilon_o}{2} \int_o^\infty E_i^2 dS \quad W_f = \frac{\epsilon_o}{2} \int_o^\infty E_f^2 dS,$$

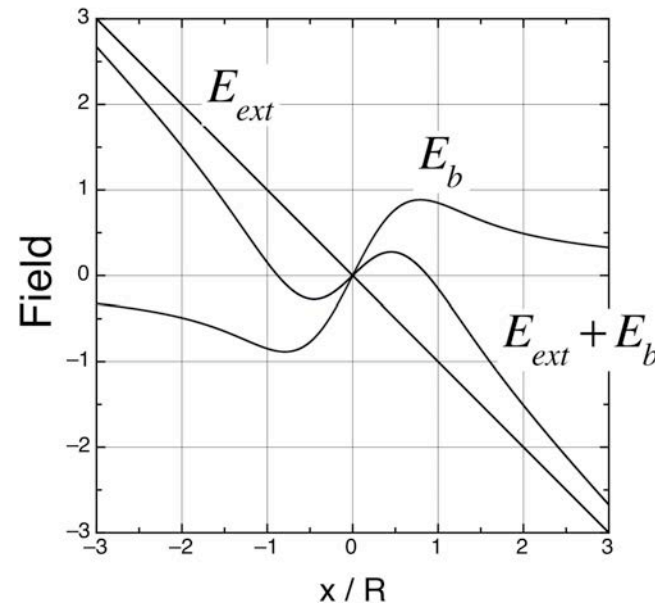
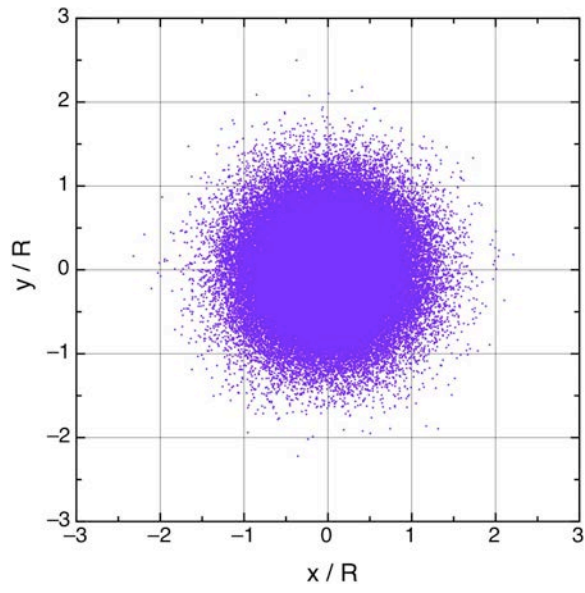
$$W_o = 2\pi\epsilon_o \left(\frac{I}{I_c} \frac{mc^2}{q\beta\gamma} \right)^2$$

and normalization constant is

Emittance Growth due to Charge Redistribution (cont.)

Consider beam with initial Gaussian distribution. Initial total field E_i is given by:

$$E_i = \frac{mc^2}{qR\gamma} \frac{2I}{\beta\gamma I_c} \left\{ -\frac{r}{R} + \frac{R}{r} \left[1 - \exp\left(-\frac{2r^2}{R^2}\right) \right] \right\}. \quad (3.73)$$

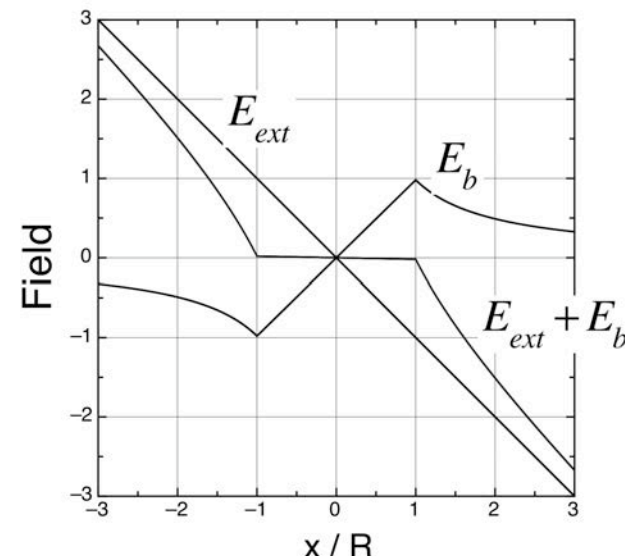
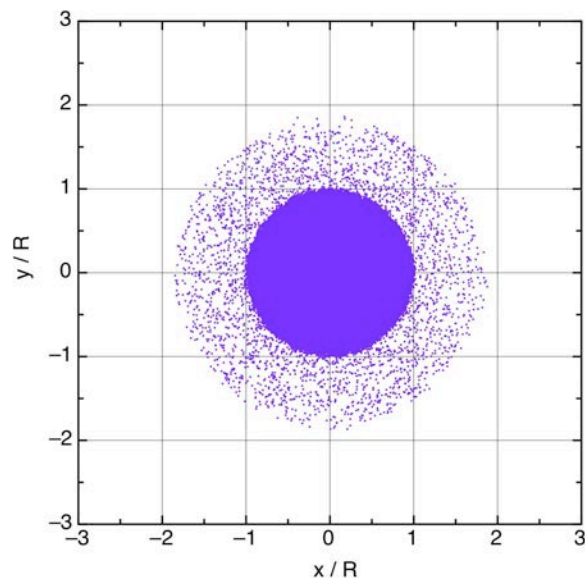


External focusing field E_{ext} , space charge field of Gaussian beam E_b , and total field $E_{ext} + E_b$ at initial moment of time.

Emittance Growth due to Charge Redistribution (cont.)

Final beam distribution is close to uniform with the same value of beam radius R . It is a general property of space-charge dominated regime, that self-field of the beam almost compensates for external field within the beam. We can put $E_f \approx 0$ within the beam and $E_f = E_{ext} + E_b$ outside the beam

$$E_f = \begin{cases} 0, & r \leq R \\ \frac{mc^2}{qR} \frac{2I}{\beta\gamma^2 I_c} \left(-\frac{r}{R} + \frac{R}{r} \right), & r > R \end{cases} . \quad (3.74)$$



External focusing field E_{ext} , space charge field E_b , and total field $E_{ext} + E_b$ after beam uniforming.

Emittance Growth due to Charge Redistribution (cont.)

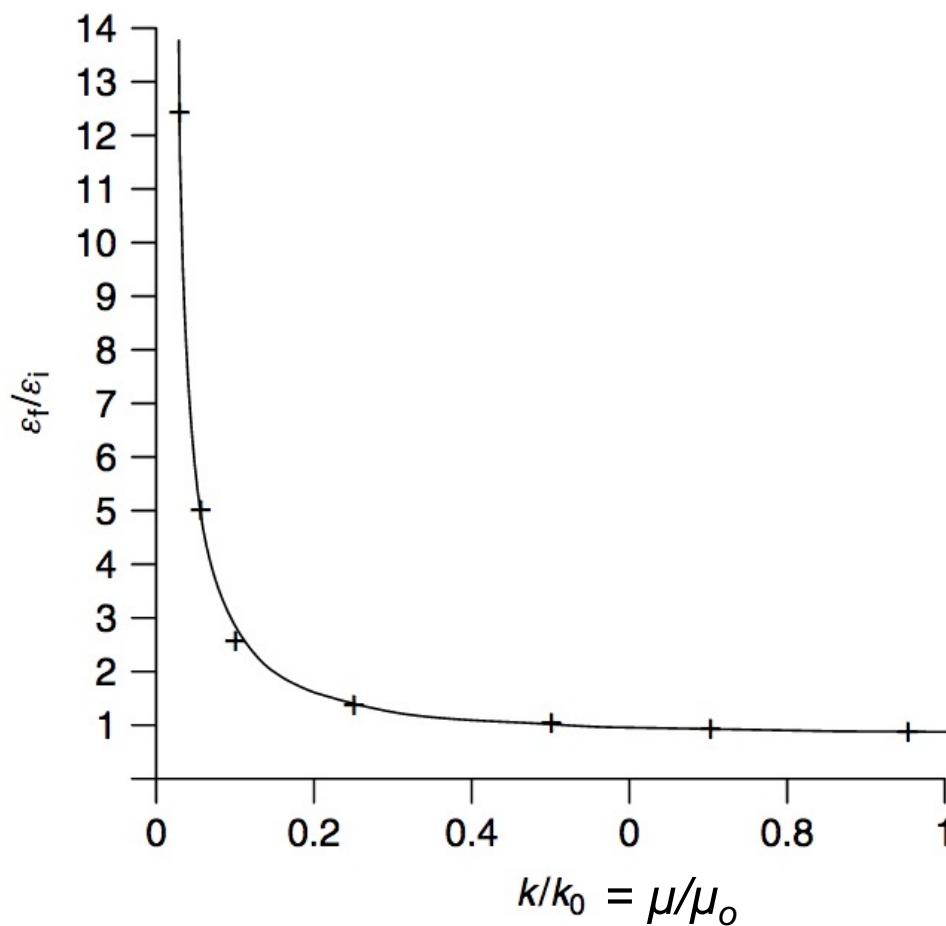
Calculation of “free energy” parameter for Gaussian beam gives:

$$\frac{W_f - W_i}{W_o} = \int_0^{\xi_{max}} \left[-\xi + \frac{1}{\xi} (1 - e^{-2\xi^2}) \right]^2 \xi d\xi - \int_1^{\xi_{max}} \left(-\xi + \frac{1}{\xi} \right)^2 \xi d\xi \approx 0.077$$

Free energy parameter for different beam distributions

4D Distribution	2D Projection	$\frac{W_i - W_f}{W_o}$
KV	ρ_o	0
Water Bag	$\rho_o \left(1 - \frac{r^2}{R^2}\right)$	0.01126
Parabolic	$\rho_o \left(1 - \frac{r^2}{R^2}\right)^2$	0.02366
Gaussian	$\rho_o \exp\left(-\frac{r^2}{R^2}\right)$	0.077

Emittance Growth due to Charge Redistribution (cont.)



Final emittance growth ratio versus space charge tune depression for an initial Gaussian beam. Typical space charge tune depression in linacs $\mu / \mu_o > 0.4$.

Excitation of Single Particle Space-Charge Induced Nonlinear Resonances

Nonlinear components of oscillating space charge field can excite nonlinear resonances. Particle dynamics in focusing channel in presence of oscillation nonlinear field is determined by equation

$$\frac{d^2x}{d\tau^2} + \mu^2 x + \alpha_n(\tau)x^{n-1} = 0$$

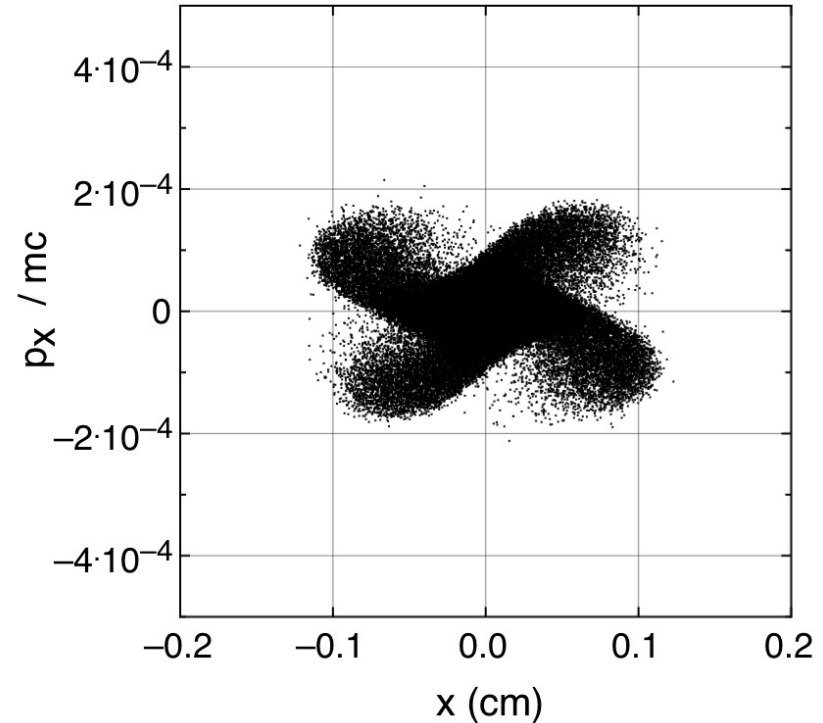
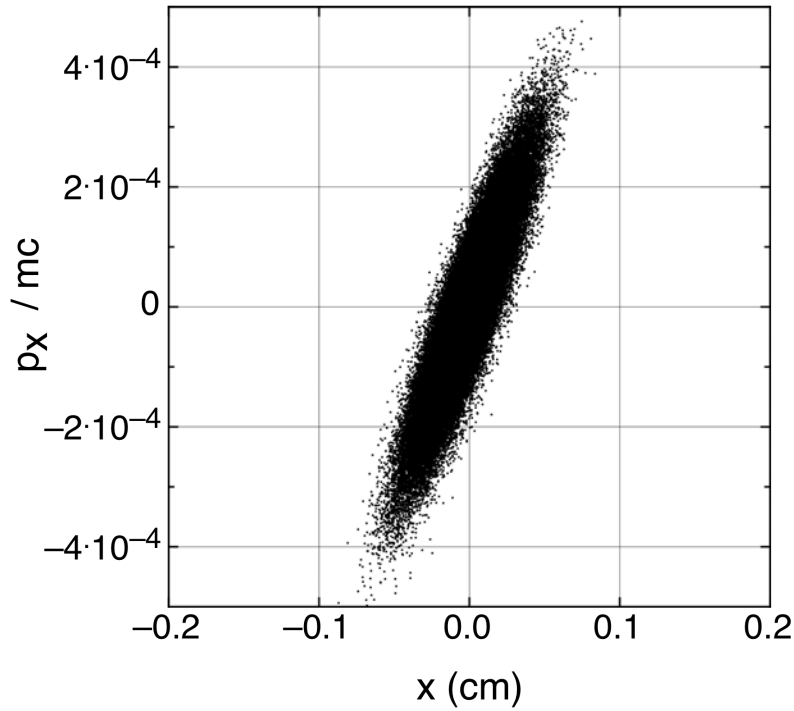
Resonance is excited when particle trajectory is perturbed integer number of times n per one complete oscillation by a nonlinear field component of the order n . The lowest-order resonance is the parametric resonance of a linear oscillator ($n = 2$) described by Mathieu equation.

Beam space charge field contains components of the order $n = 2, 4, 6, \dots$ Beam envelope oscillates with the period of focusing structure and constitute periodic perturbation of single-particle trajectory. Resonance condition for excitation of single particle nonlinear resonances:

$$\mu = \frac{360^\circ}{n}, \quad n = 2, 3, 4, \dots$$

Single Particle Nonlinear Resonance of the 4th Order ($n = 4$)

Space-charge induces single-particle resonance of the 4th order in channels with $\mu = 360^\circ / 4$ (D. Jeon et al, PRSTAB 2009). Because phase advance in presence of space charge forces is $\mu = \mu_s - \Delta\mu$, this resonance of the 4th order can be excited only in channels with $\mu_s > 90^\circ$ and $\mu_t < 90^\circ$. Accelerators are typically designed with $\mu_s < 90^\circ$ to avoid envelope resonances, and this 4th order resonance is not excited when $\mu_s < 90^\circ$.



Excitation of nonlinear resonance of the 4th order in accelerator channel with $\mu_s = 93^\circ$, $\mu_t = 63^\circ$.

73

Experimental Observation of Space-Charge Driven Resonance of 4th Order in Linac (L. Groening et al, LINAC2010)

Matched beam envelope

$$R(s, \sigma_{env}) = R_o(\sigma_{env}) + \Delta R(\sigma_{env}) \cdot \cos(\sigma_{env}s)$$

Radial electric field

$$E_r = \frac{18 \cdot I}{\pi \epsilon_0 \cdot R(s)^2 \beta c} \left[r - \frac{r^3}{2R(s)^2} + O(r) \right]$$

Single-particle trajectory

$$r'' = -\sigma_{\perp,o}^2 r + \frac{e \cdot q}{A \cdot m_u} \cdot E_r$$

or

Disturbed oscillator with σ_{\perp} as depressed phase advance

$$r'' + \sigma_{\perp}^2 r \sim |r^3| \cdot e^{i\sigma_{env}s}$$

Resonance condition:

$$\sigma_{env} = 4\sigma_{\perp}$$

Phase advance of the matched envelope is 360°, the resonance occurs at $\sigma_{\perp} = 90^\circ$

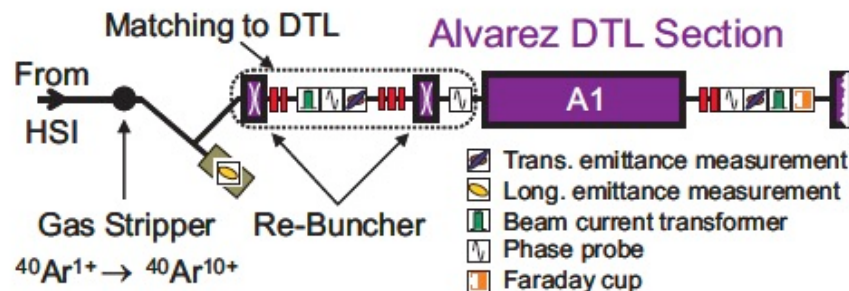


Figure 3: Schematic set-up of the experiments (not to scale).

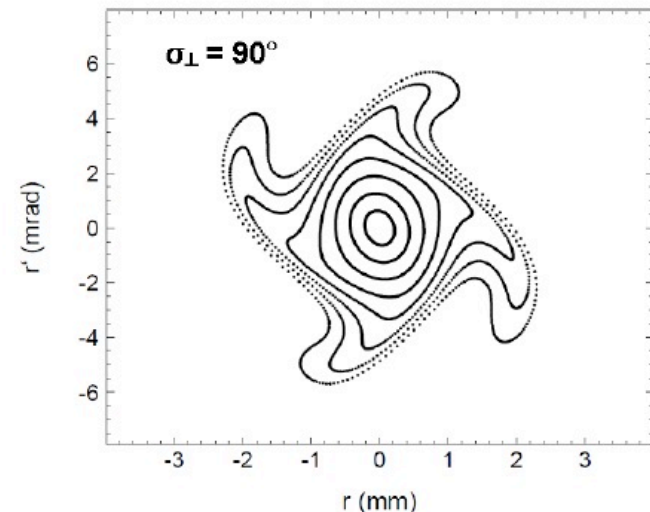


Figure 1: Distribution of particles at the exit of the periodic channel according to the radial particle-core model of the space charge driven transverse 4th-order resonance.

Experimental Observation of Space-Charge Driven Resonances (cont.)

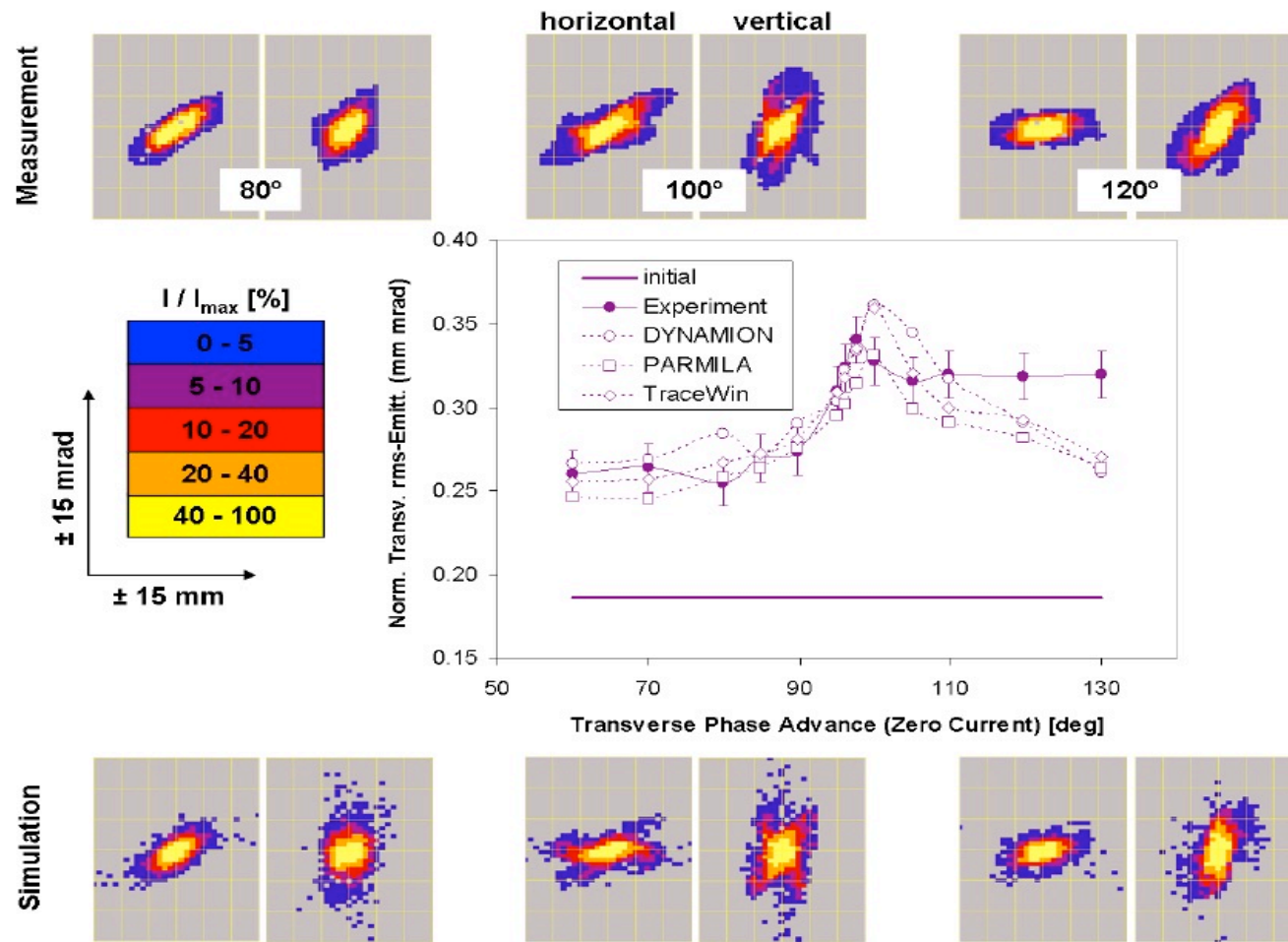
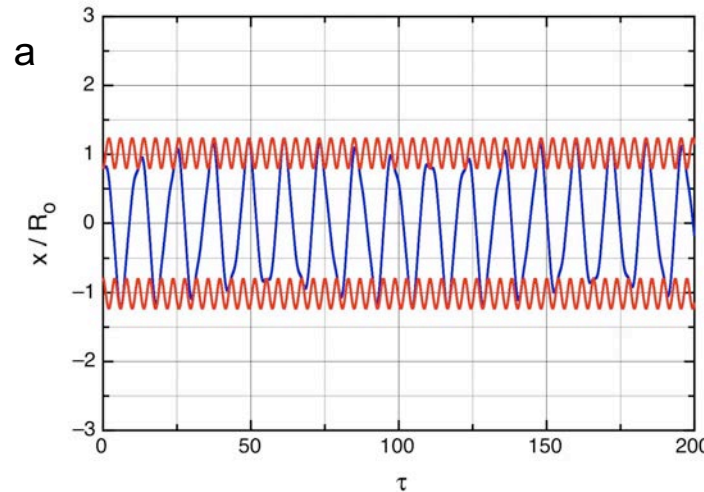
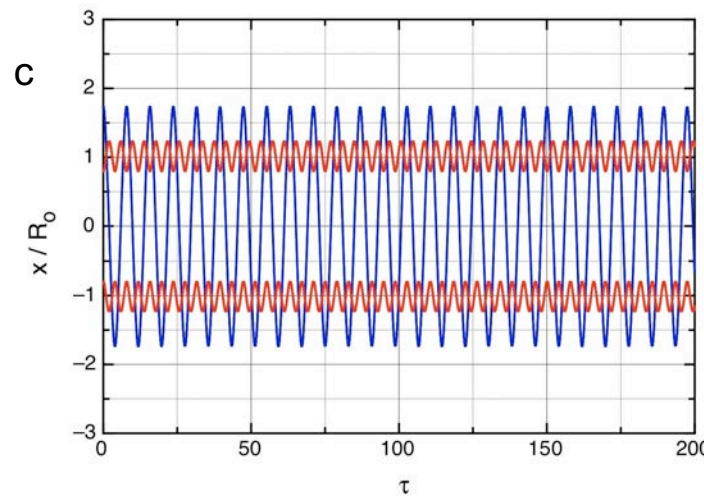


Figure 7: Upper and lower: phase space distributions at the exit of the first DTL tank as obtained from measurements and from the DYNAMION code for phase advances $\sigma_{\perp,o}$ of 80°, 100°, and 120°. Left (right) side distributions refer the horizontal (vertical) plane. The scale is ± 15 mm and ± 15 mrad. Fractional intensities refer to the phase space element including the highest intensity. Center: Mean of horizontal and vertical normalized rms emittance behind the first DTL tank as a function of the transverse zero current phase advance.

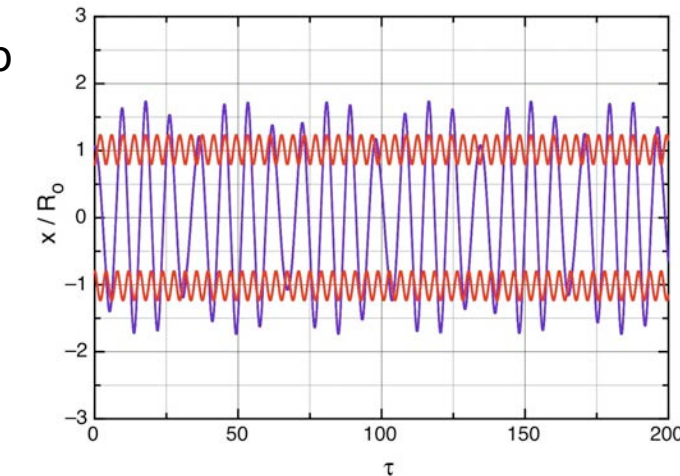
Halo Development in Particle-Core Interaction



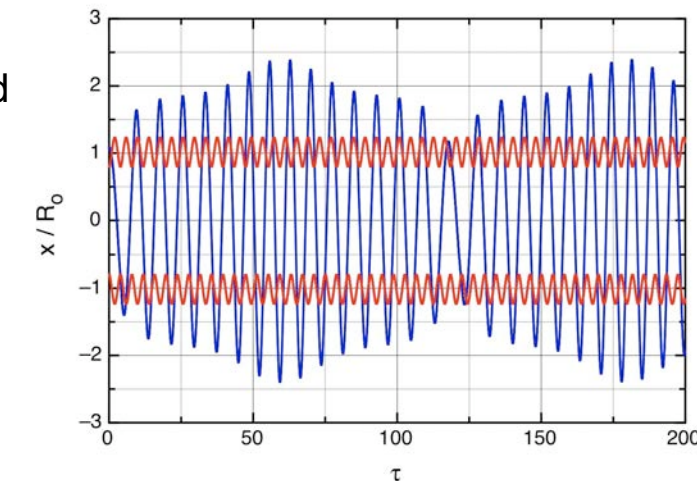
$$\frac{x_o}{R_o} = 0.8$$



$$\frac{x_o}{R_o} = 1.728$$



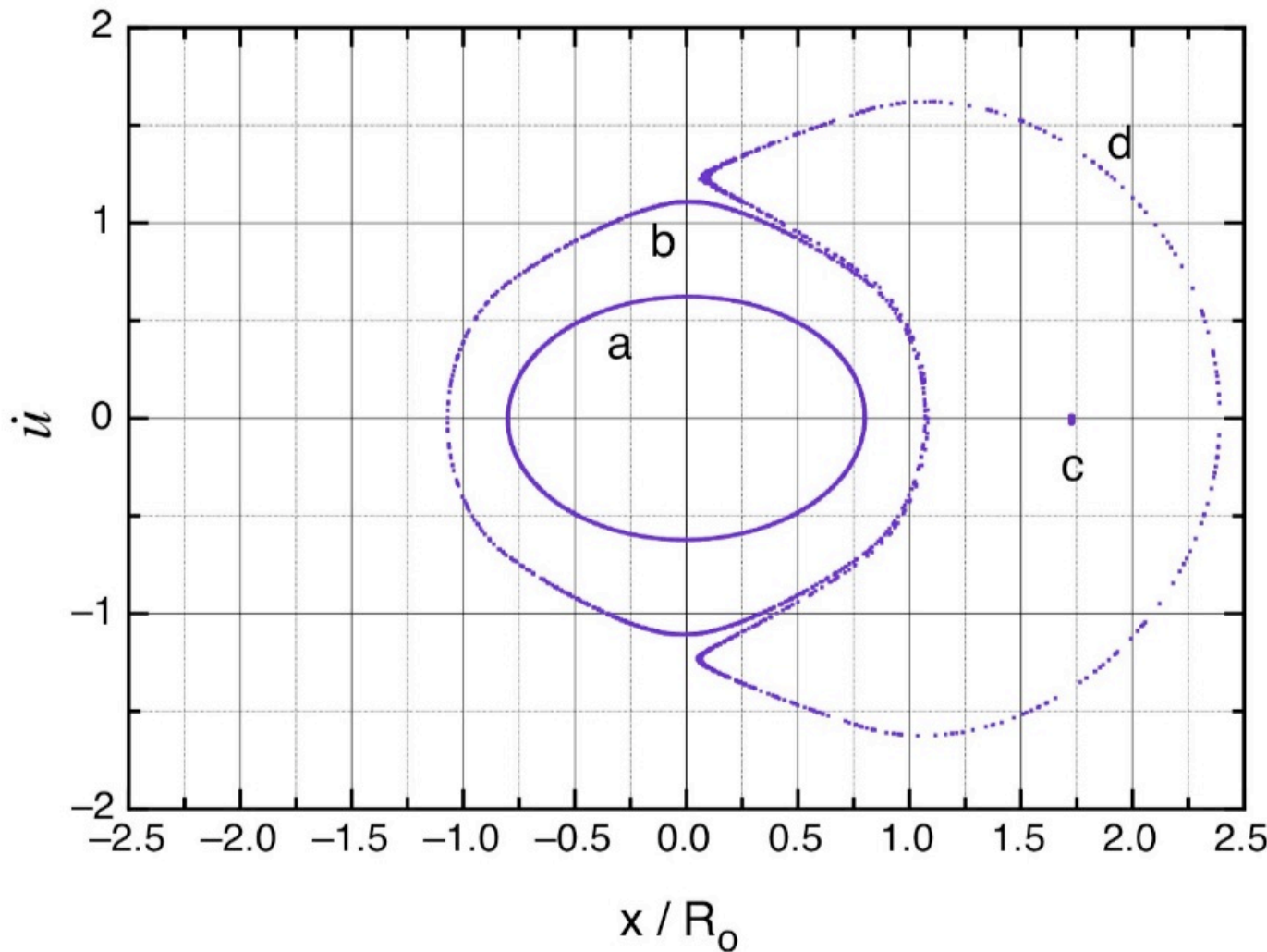
$$\frac{x_o}{R_o} = 1.071$$



$$\frac{x_o}{R_o} = 1.082$$

Envelope oscillations of the beam with space charge parameter $b=3$, amplitude $\Delta=0.2$ and single particle trajectories with initial conditions (a) $x_o/R_o=0.8$, (b) $x_o/R_o =1.071$, (c) $x_o/R_o =1.728$, (d) $x_o/R_o =1.082$.

Stroboscopic Particle Motion



Stroboscopic particle trajectories at phase plane $(u, du / d\tau)$ taken after each two envelope oscillation periods: (a) $x_o/R_o=0.8$, (b) $x_o/R_o=1.071$, (c) $x_o/R_o=1.728$, (d) $x_o/R_o=1.082$.

Particle – Core Model

Dimensionless $r = \frac{R}{R_e}$ beam envelope (core) equation: $\frac{d^2r}{d\tau^2} + r - \frac{1}{(1+b)r^3} - \frac{b}{(1+b)r} = 0$

Single particle equation of motion $u = \frac{x}{R_e}$

$$\frac{d^2u}{d\tau^2} + u = \begin{cases} \frac{b}{(1+b)r^2}, & |u| \leq r \\ \frac{b}{(1+b)u}, & |u| > r \end{cases}$$

Space charge parameter

$$b = \frac{2}{\beta\gamma} \frac{I}{I_c} \frac{R_e^2}{\epsilon^2}$$

I beam current

$I_c = 4\pi\epsilon_0 mc^3 / q$ characteristic beam current

ϵ normalized beam emittance

β particles velocity,

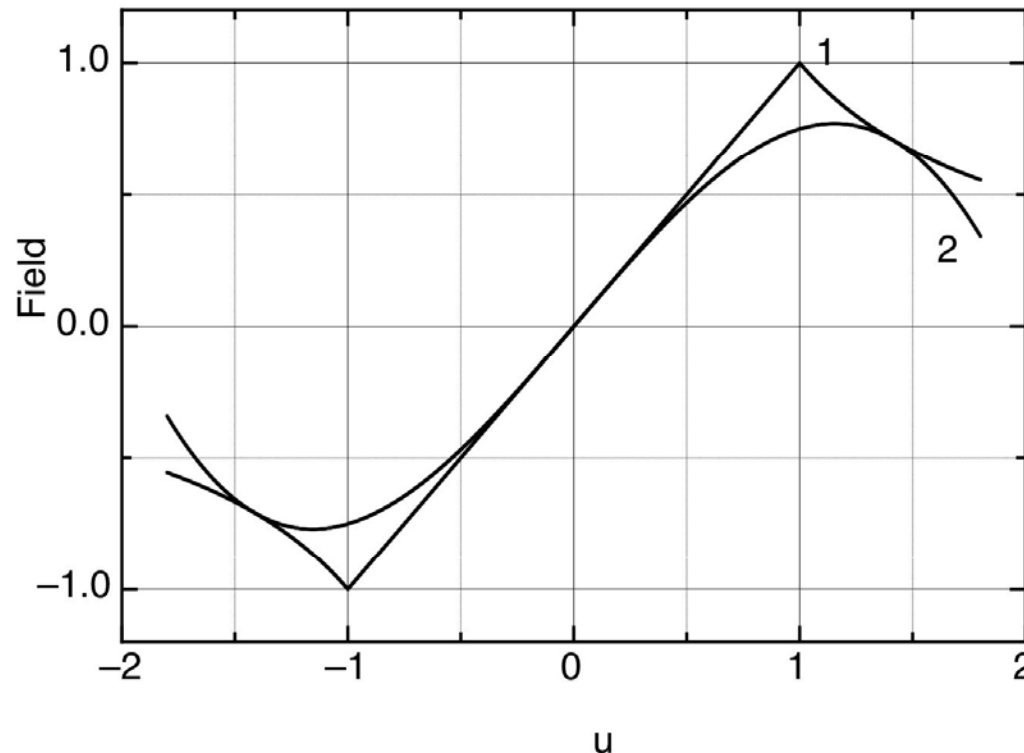
γ particle energy

R_e radius of the equilibrium envelope

Small intensity beam $b \approx 0$

High intensity beam $b \gg 1$

Approximation of Space Charge Field



(1) Field of uniformly charged beam

$$F = \frac{b}{(1+b)} \begin{cases} \frac{u}{r^2}, & |u| \leq r \\ \frac{1}{u}, & |u| > r \end{cases}$$

(2) Field approximation:

$$F = \frac{b}{(1+b)} \left(-\frac{u}{r^2} + \frac{u^3}{4} \right)$$

Mismatched Envelope Oscillation

Envelope equation

$$\frac{d^2r}{d\tau^2} + r - \frac{1}{(1+b)r^3} - \frac{b}{(1+b)r} = 0$$

Expansions

$$r = 1 + \vartheta \quad \frac{1}{r} \approx 1 - \vartheta \quad \frac{1}{r^3} \approx 1 - 3\vartheta$$

$$\frac{d^2\vartheta}{d\tau^2} + 2\left(\frac{2+b}{1+b}\right)\vartheta = 0$$

Equation for small deviation from equilibrium

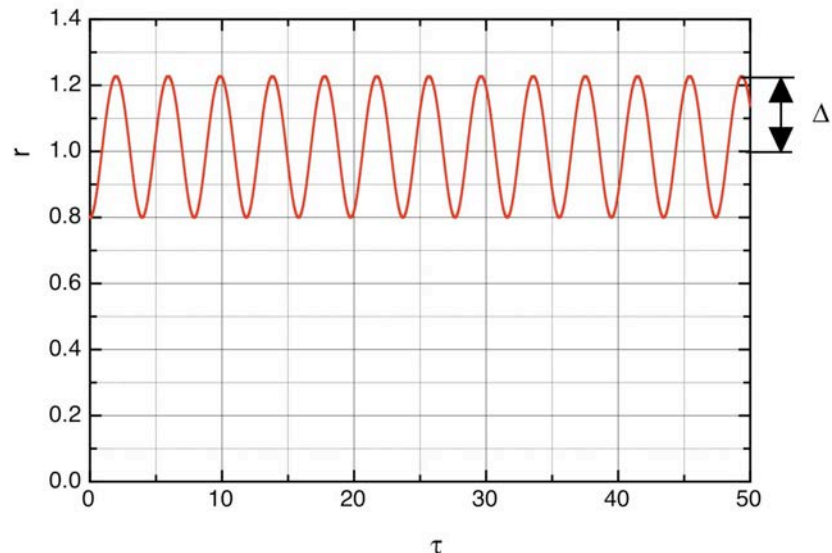
$$r = 1 + \Delta \cos(2\Omega\tau)$$

Envelope oscillation frequency

$$2\Omega = \sqrt{2\left(\frac{2+b}{1+b}\right)}$$

For small intensity beam $b \approx 0$ $r = 1 + \Delta \cos 2\tau$

For high intensity beam $b \gg 1$ $r = 1 + \Delta \cos \sqrt{2}\tau$



Harmonic Oscillator with Parametric Excitation for Single Particle Motion

With field approximation, equation of particle motion is

$$\frac{d^2u}{d\tau^2} + u - \left(\frac{b}{1+b}\right) \left[\frac{u}{(1+\Delta\cos 2\Omega\tau)^2} - \frac{u^3}{4} \right] = 0$$

Using expansion

$$\frac{1}{(1+\Delta\cos 2\Omega\tau)^2} \approx 1 - 2\Delta\cos 2\Omega\tau$$

Equation of particle motion

$$\frac{d^2u}{d\tau^2} + u \left(\frac{1}{1+b} \right) (1 + 2b\Delta\cos 2\Omega\tau) + \left(\frac{b}{1+b} \right) \frac{u^3}{4} = 0$$

Equation corresponds to Hamiltonian

$$H = \frac{\dot{u}^2}{2} + \varpi^2 \frac{u^2}{2} (1 - h\cos 2\Omega\tau) + \alpha \frac{u^4}{4}$$

with the following notations

$$\varpi^2 = \frac{1}{1+b} \quad h = -2b\Delta \quad \alpha = \frac{b}{4(1+b)}$$

Canonical Transformation of Hamiltonian

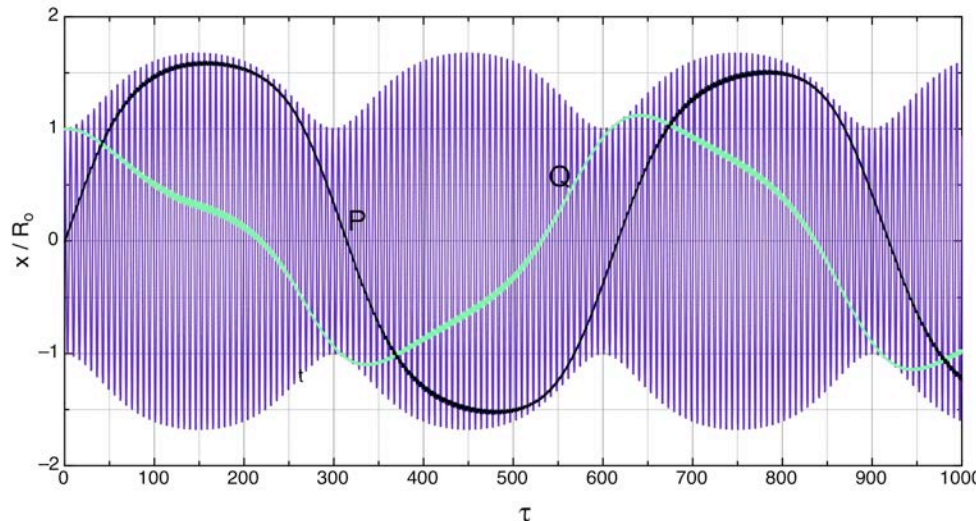
Change the variables (\dot{u}, u) to new variables (Q, P) using a generating function

$$F_2(u, P, \tau) = \frac{uP}{\cos \Omega \tau} - \left(\frac{P^2}{2\bar{\omega}} + \bar{\omega} \frac{u^2}{2} \right) \operatorname{tg} \Omega \tau$$

Relationships between variables are given by:

$$\begin{cases} Q = \frac{\partial F_2}{\partial P} = \frac{u}{\cos \Omega \tau} + \frac{P}{\bar{\omega}} \operatorname{tg} \Omega \tau \\ \dot{u} = \frac{\partial F_2}{\partial u} = \frac{P}{\cos \Omega \tau} - \bar{\omega} u \operatorname{tg} \Omega \tau \end{cases}$$

or $\begin{cases} u = Q \cos \Omega \tau + \frac{P}{\bar{\omega}} \sin \Omega \tau \\ \dot{u} = -\bar{\omega} Q \sin \Omega \tau + P \cos \Omega \tau \end{cases}$



Averaged Hamiltonian

New Hamiltonian

$$K = H + \frac{\partial F_2}{\partial \tau}$$

$$K = \frac{P^2}{2} + \bar{\omega}^2 \frac{Q^2}{2} - \frac{\bar{\omega}^2 h}{2} (Q \cos \Omega \tau + \frac{P}{\bar{\omega}} \sin \Omega \tau)^2 \cos 2\Omega \tau + \frac{\alpha}{4} (Q \cos \Omega \tau + \frac{P}{\bar{\omega}} \sin \Omega \tau)^4 - \frac{P^2 \Omega}{2\bar{\omega}} - \frac{\Omega \bar{\omega}}{2} Q^2$$

After averaging all time-dependent terms over period of $2\pi/\Omega$

$$\bar{K} = \frac{\bar{\omega}^2 \bar{Q}^2}{2} \left(1 - \frac{\Omega}{\bar{\omega}} - \frac{h}{4}\right) + \frac{\bar{P}^2}{2} \left(1 - \frac{\Omega}{\bar{\omega}} + \frac{h}{4}\right) + \frac{3}{32} \alpha \left(\bar{Q}^2 + \frac{\bar{P}^2}{\bar{\omega}^2}\right)^2$$

Second Canonical Transformation

Change variables (\bar{Q}, \bar{P}) to action-angle variables (J, ψ) using generating function

$$F_1(\bar{Q}, \psi) = \frac{\varpi \bar{Q}^2}{2t g \psi}$$

$$\begin{cases} \bar{Q} = \sqrt{\frac{2J}{\varpi}} \sin \psi \\ \bar{P} = \sqrt{2J\varpi} \cos \psi \end{cases}$$

Transformation is given by

New Hamiltonian

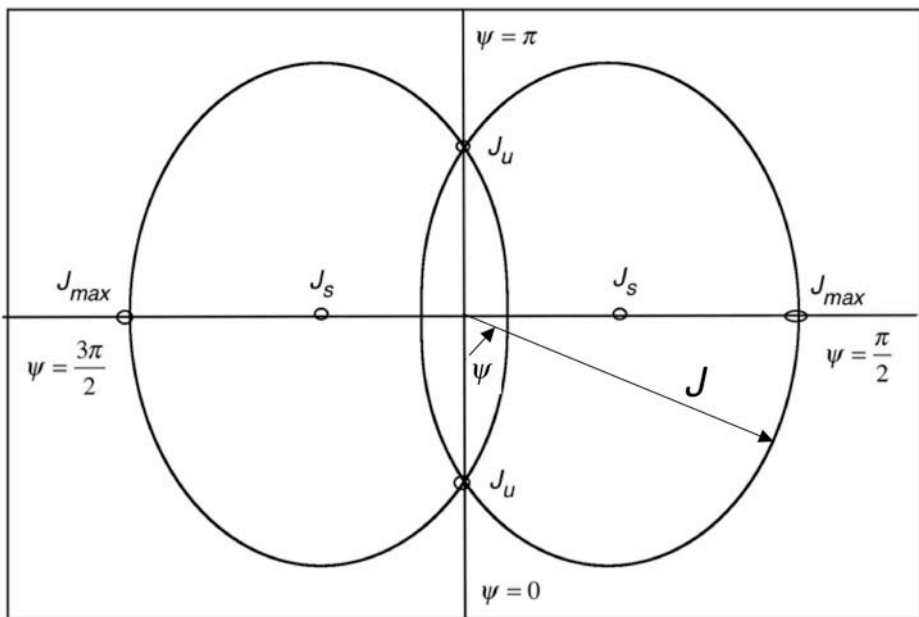
$$\boxed{\bar{K} = vJ + \kappa J^2 + 2\chi J \cos 2\psi}$$

with the following notations

$$v = \varpi - \Omega = \frac{\sqrt{2} - \sqrt{2+b}}{\sqrt{2(1+b)}} \quad \kappa = \frac{3}{32}b \quad \chi = -\frac{1}{4} \frac{b\Delta}{\sqrt{1+b}}$$

Nonlinear Parametric Resonance

Hamiltonian of averaged motion:



$$\bar{K} = vJ + \kappa J^2 + 2\chi J \cos 2\psi$$

Maximum deviation of particle from the axis

$$\frac{x_{\max}}{R_e} = \sqrt{\frac{2J_{\max}}{\omega}}$$

$$J_{\max} = \frac{(-v + 2\chi) + \sqrt{8|v\chi|}}{2\kappa}$$

$$\frac{x_{\max}}{R_e} = \sqrt{\frac{32}{3} \frac{\sqrt{1 + \frac{b}{2}} - 1 + \frac{b|\Delta|}{2}}{b} + \sqrt{2b|\Delta|(\sqrt{1 + \frac{b}{2}} - 1)}}$$

Nonlinear Parametric Resonance

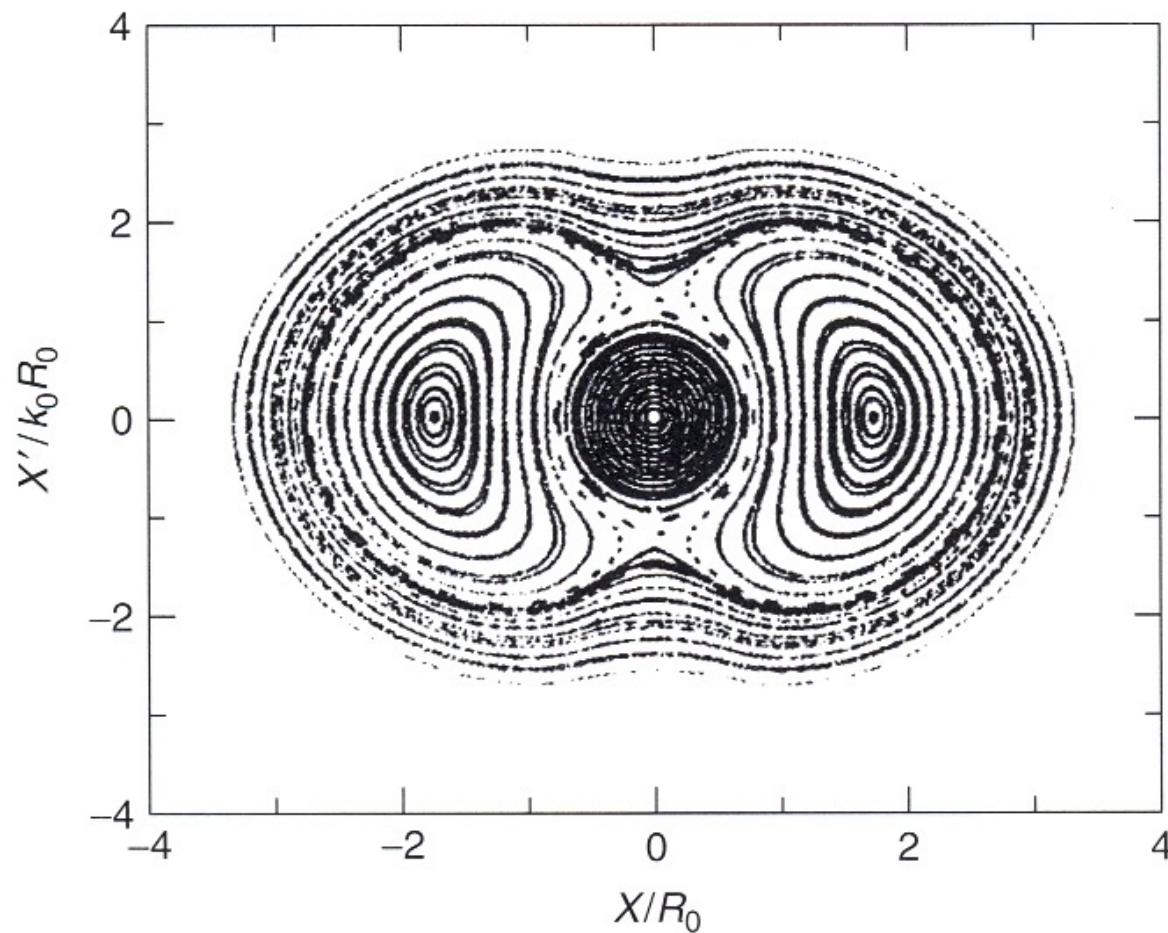
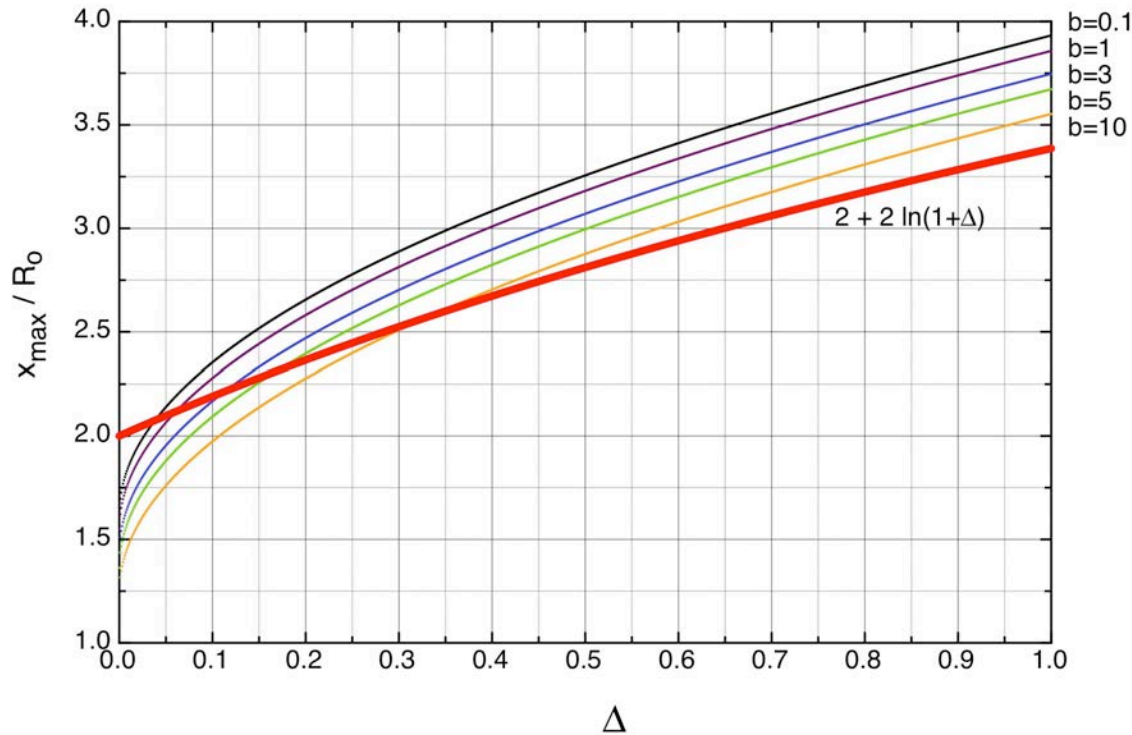


Figure 9.12 Stroboscopic plot obtained by taking snapshots of many independent particle trajectories, once per core-oscillation cycle at the phase of the

core oscillation that gives the minimum core radius. Initial particle coordinates were defined on the x and x' axes.

Comparison of Analytical and Numerical Results

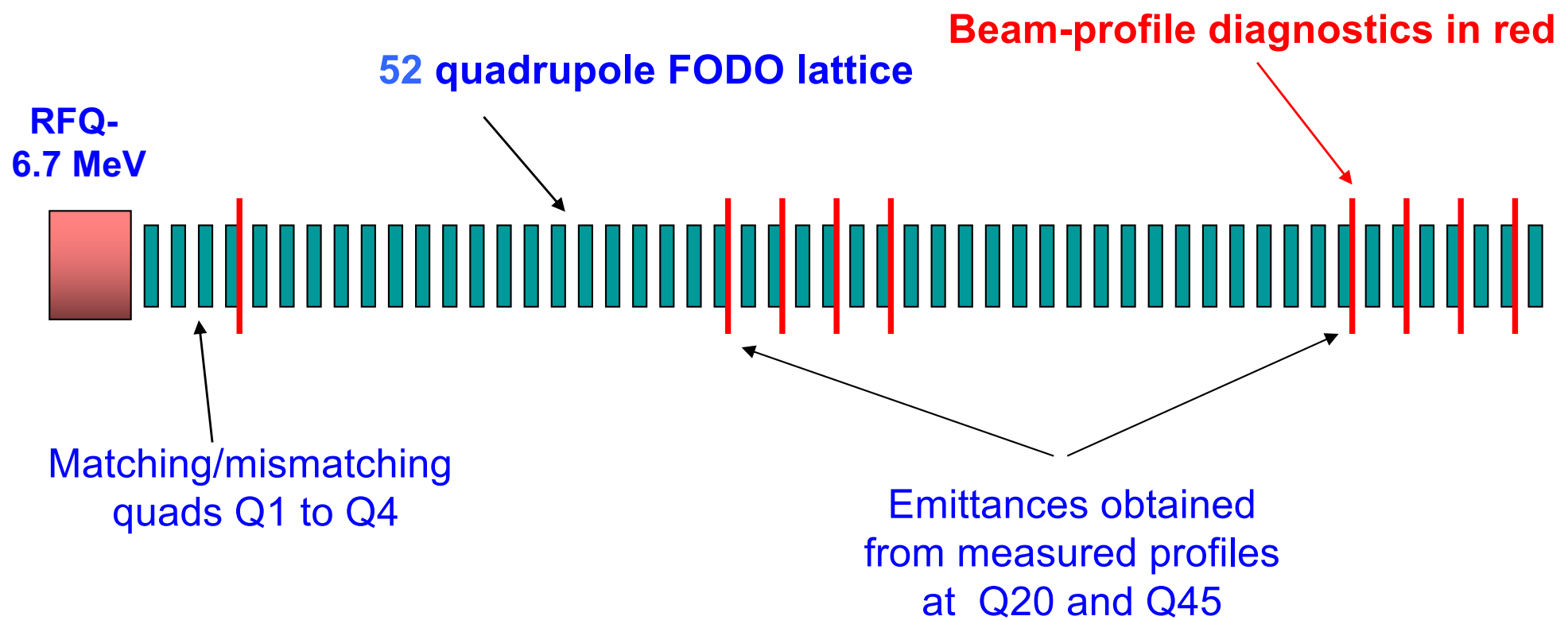


Maximum values of particle deviation from the axis as a function of amplitude of core oscillations (Y.B. NIM-A 618, 2010, p.37). (Red) model of Tom Wangler (*RF Linear Accelerators*, Wiley, 1998)

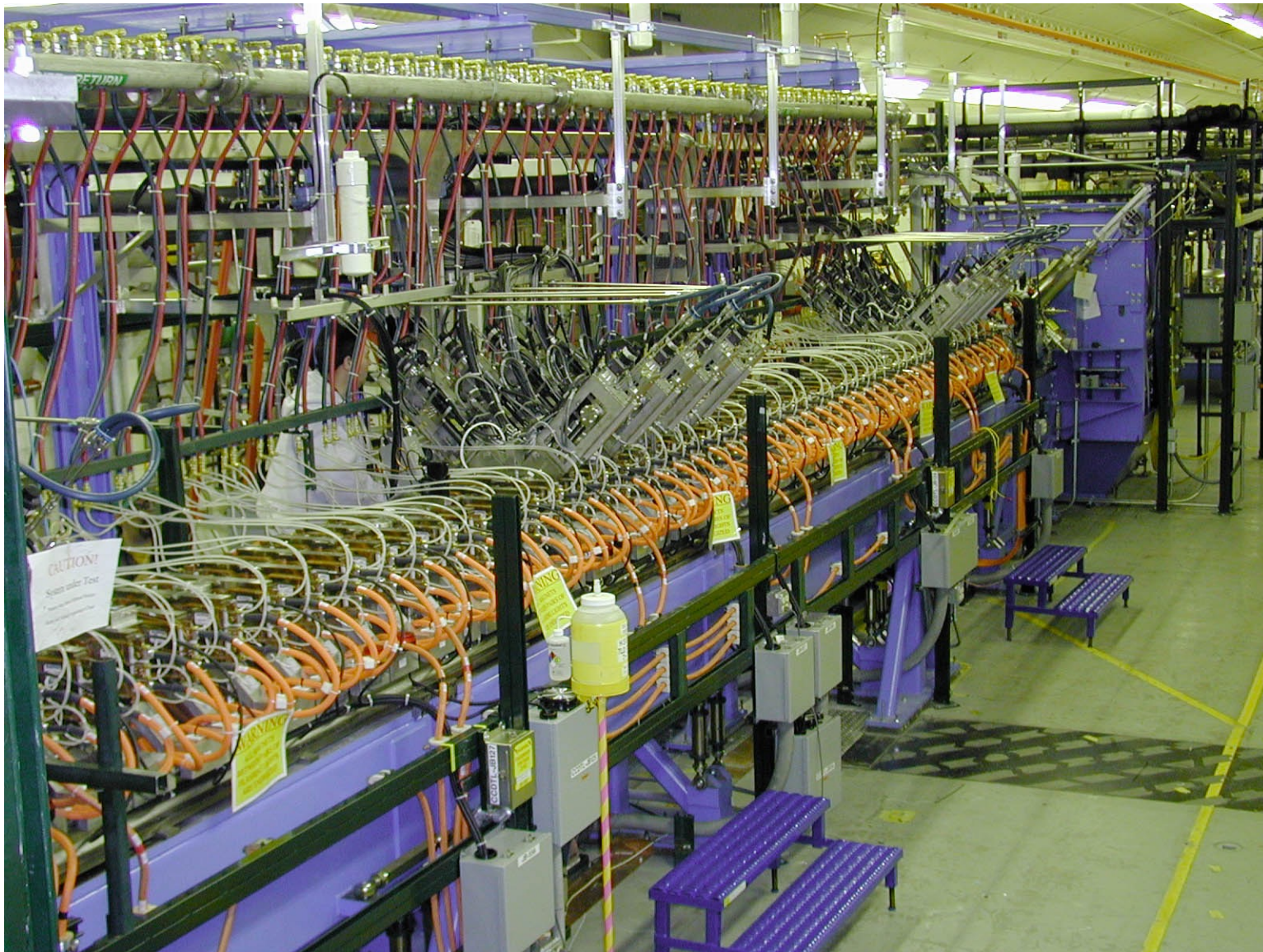
$$\frac{x_{\max}}{R_o/2} = A + B \ln(\mu)$$

where $A = B = 4$, $\mu = 1 + \Delta$.

LANL Beam Halo Experiment (2002)

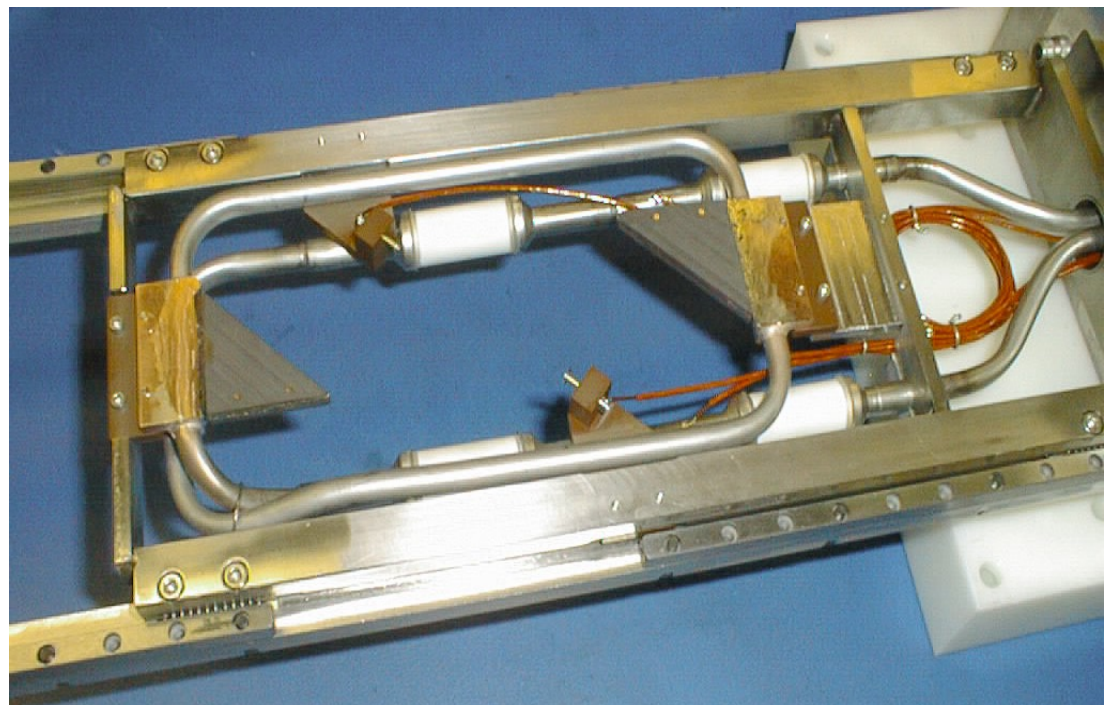


LANL Beam Halo Experiment Lattice



Wire and Scraper Beam-Profile Diagnostic to Measure Beam Profile

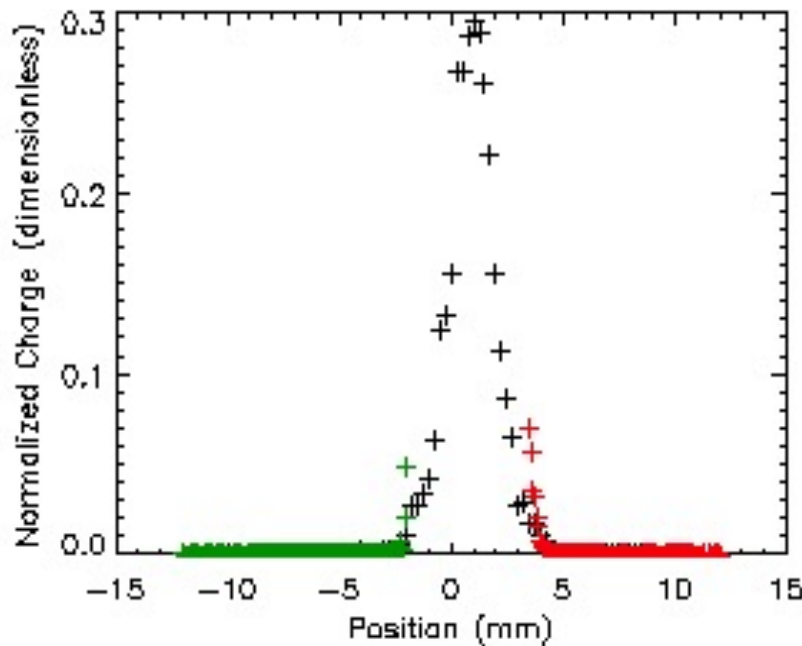
- 33-micron carbon wire (too thin to be visible in picture) measures density in beam core above 10^{-3} level.
- Proton range=300 microns so protons pass through wire and make secondary electrons to measure high density in beam core.
- Pair of 1.5mm graphite scraper plates in which protons stop. Can measure proton density outside beam core from 10^{-3} to 10^{-5} .
- Data from wire and scraper plates were combined to produce a single distribution.



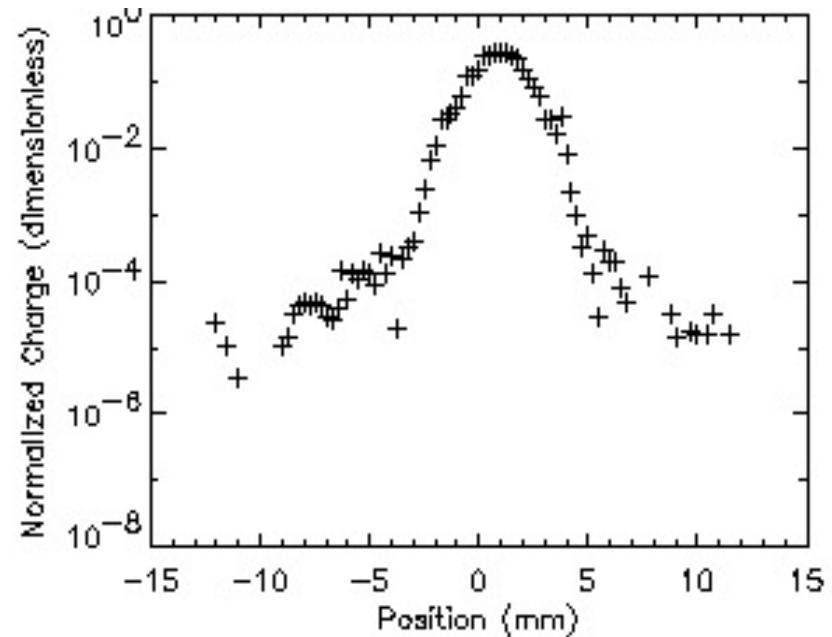
Measured Beam Profile

Typical matched beam profile for 75 mA. ($\mu=1$,matched)
Shows Gaussian-like core plus low-density halo input beam, observed
out to 9 rms.

Linear Plot

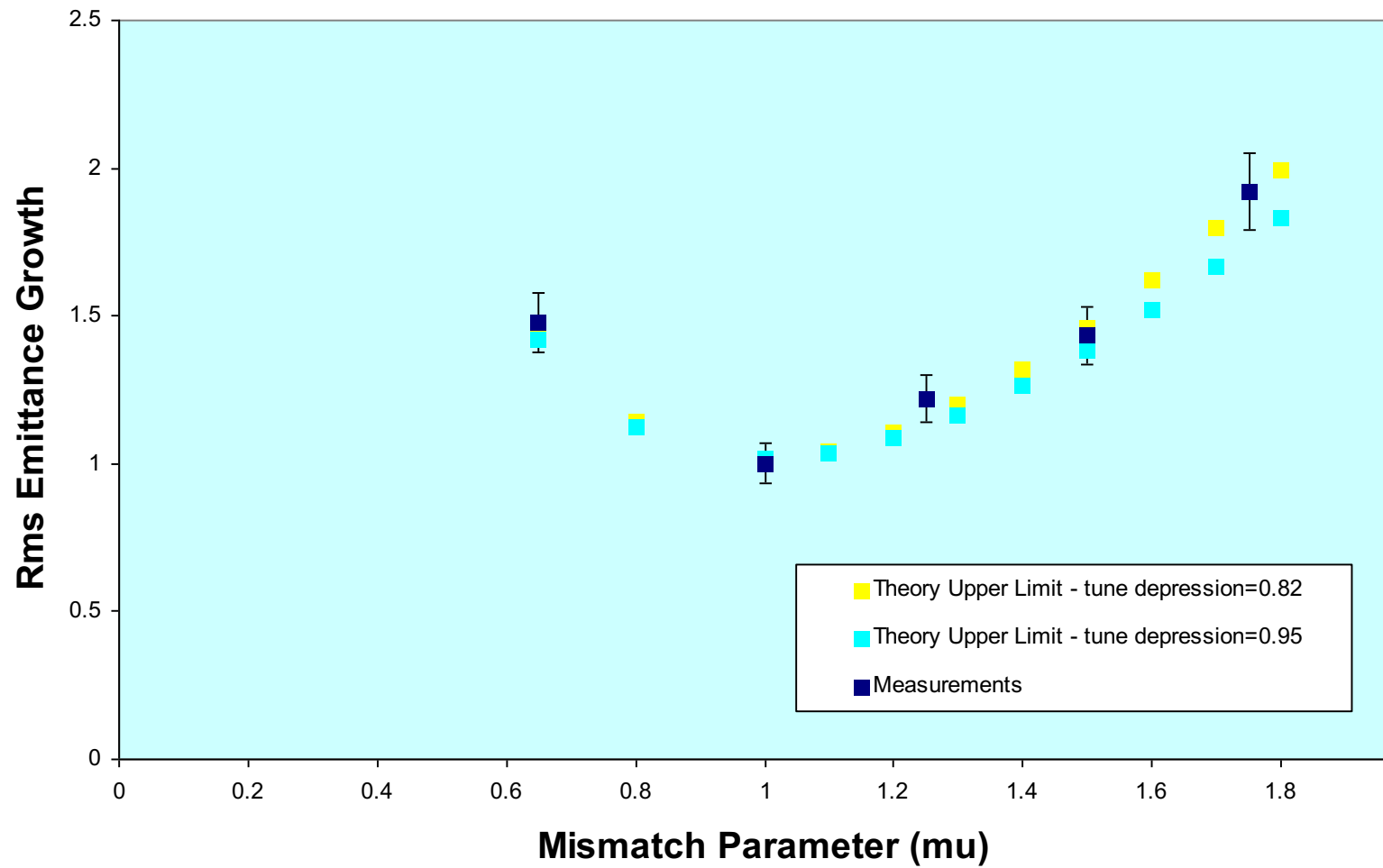


Semilog Plot



Beam Emittance Growth

RMS EMITTANCE GROWTH AT SCANNER #20 - 75 mA - BREATHING MODE

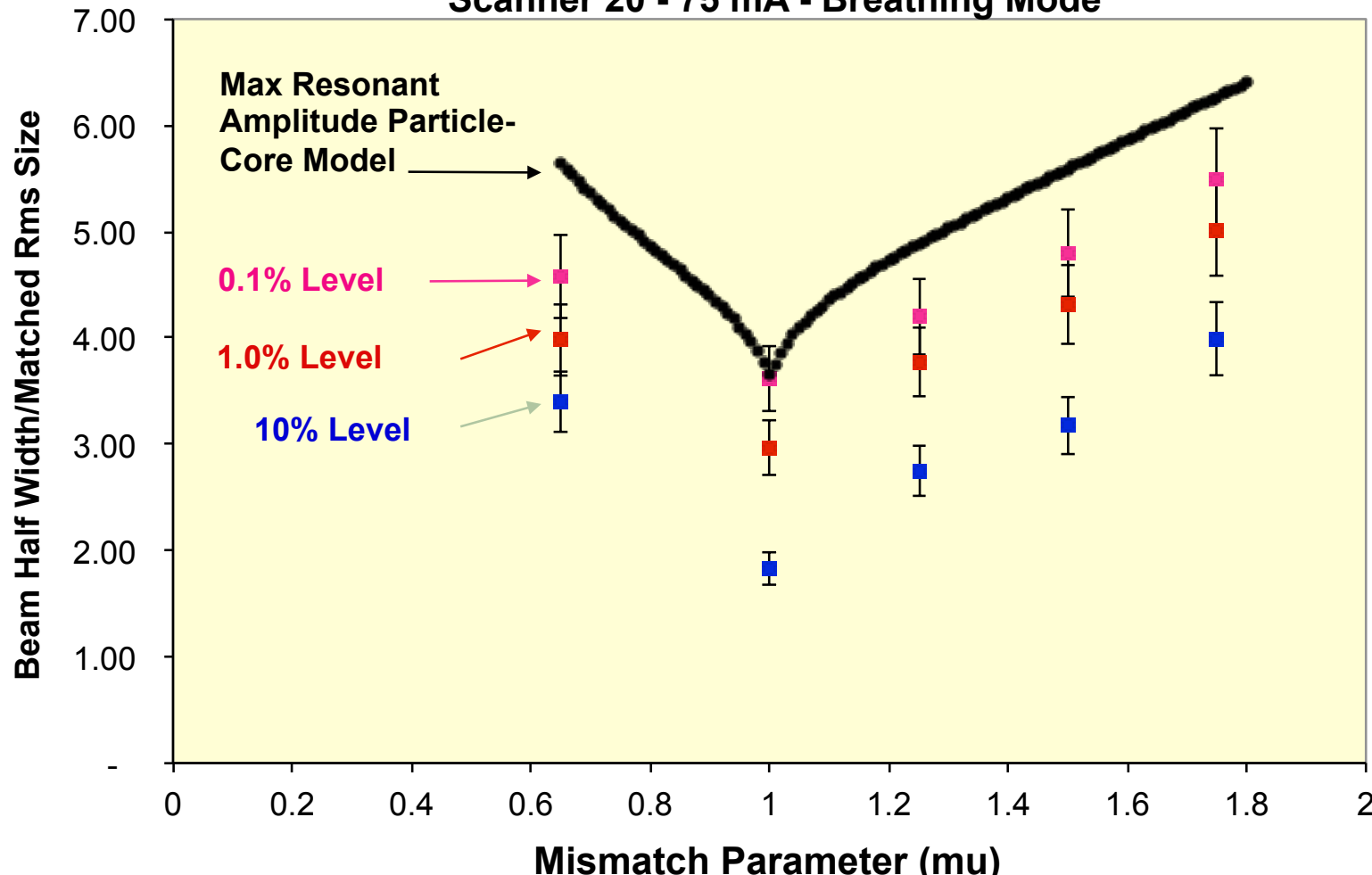


Test of Particle-Core Model

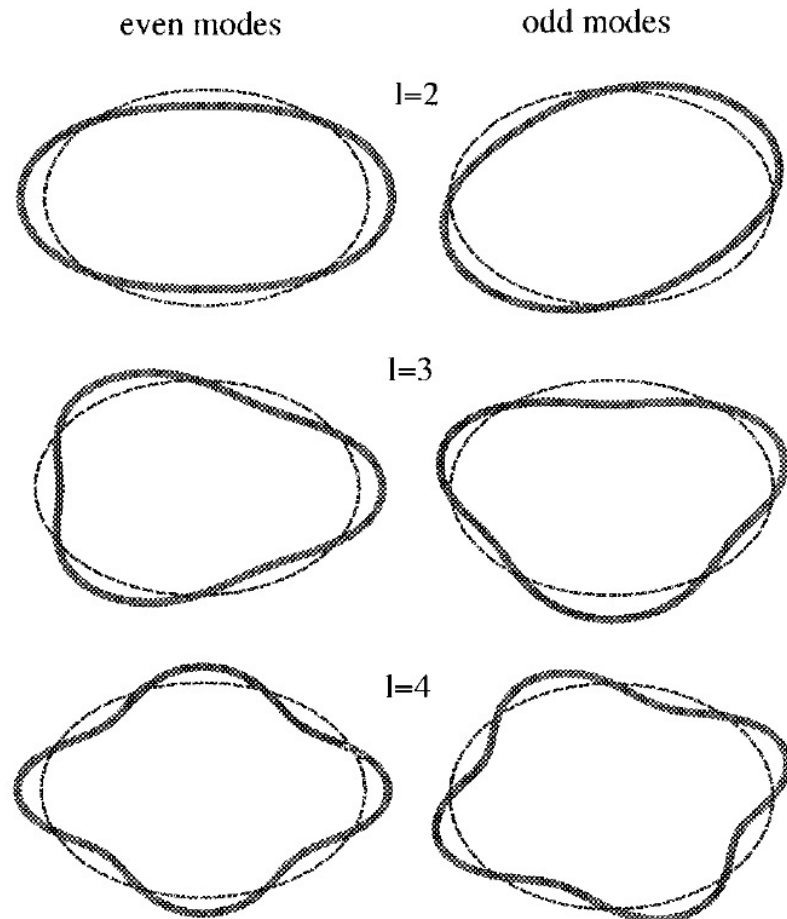
Measurements at Different Fractional Intensity Levels (10%, 1%, 0.1%)

Comparison of Measured Beam Widths With Maximum Amplitude
From Particle-Core Model

Scanner 20 - 75 mA - Breathing Mode



Instability of Anisotropic KV Beam



KV Beam with unequal emittances in a focusing channel with different focusing strength in x- and y- directions

$$f_0(x,y,p_x,p_y) = \frac{NT\nu_y/\nu_x}{2\pi^2 m \gamma a^2} \delta(H_{0x} + TH_{0y} - m\gamma\nu_x^2 a^2/2)$$

Ratio of beam emittances:

$$\frac{\epsilon_x}{\epsilon_y} = \frac{a^2 \nu_x}{b^2 \nu_y}$$

Beam cross sections for second, third and fourth order even and odd modes ~schematic, with x horizontal and y vertical coordinates.

(I.Hofmann, 1998)

94

Instability of Anisotropic KV Beam (cont.)

Perturbed distribution function

$$f \equiv f_0(H_{0x}, H_{0y}) + \hat{f}_1(x, y, p_x, p_y, t)$$

Vlasov's equation for perturbed beam distribution function

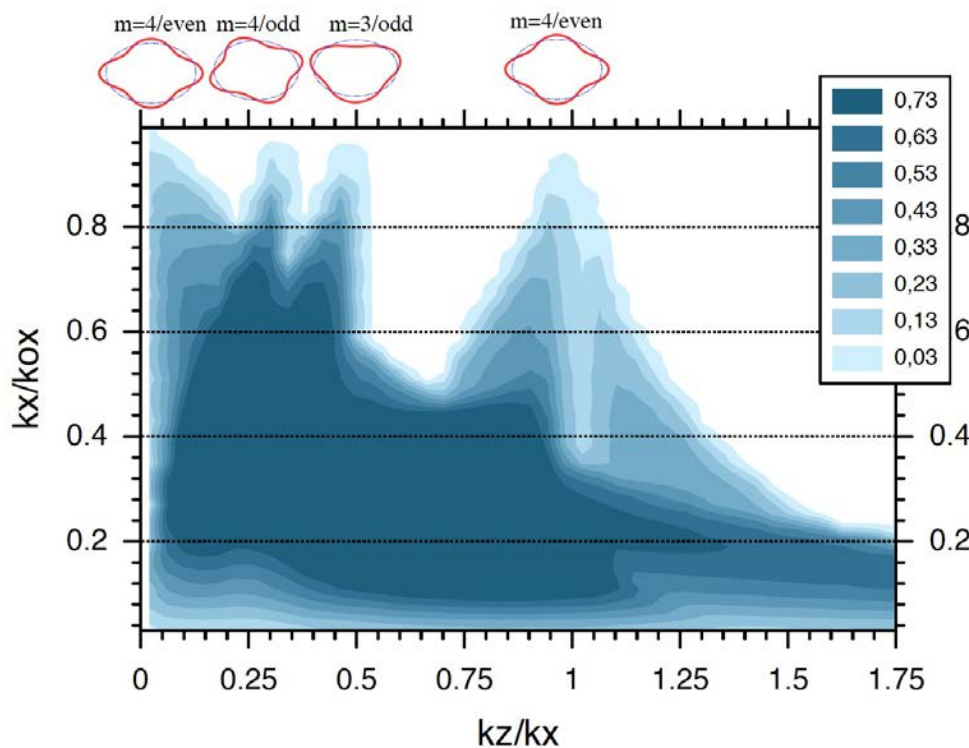
$$\begin{aligned} \frac{df_1}{dt} &\equiv \frac{\partial f_1}{\partial t} + \frac{p_x}{m\gamma} \frac{\partial f_1}{\partial x} + \frac{p_y}{m\gamma} \frac{\partial f_1}{\partial y} - m\gamma\nu_x^2 x \frac{\partial f_1}{\partial p_x} - m\gamma\nu_y^2 y \frac{\partial f_1}{\partial p_y} \\ &= \frac{NTq\nu_y/\nu_x}{2\pi^2 m^2 \gamma^4 a^2} \left(p_x \frac{\partial \Phi}{\partial x} + T p_y \frac{\partial \Phi}{\partial y} \right) \\ &\quad \times \delta' [p_x^2 + \nu_x^2 x^2 + T(p_y^2 + \nu_y^2 y^2) - \nu_x^2 a^2]. \end{aligned} \quad (11)$$

Poisson's equation for perturbed electrostatic potential created by perturbed space charge density

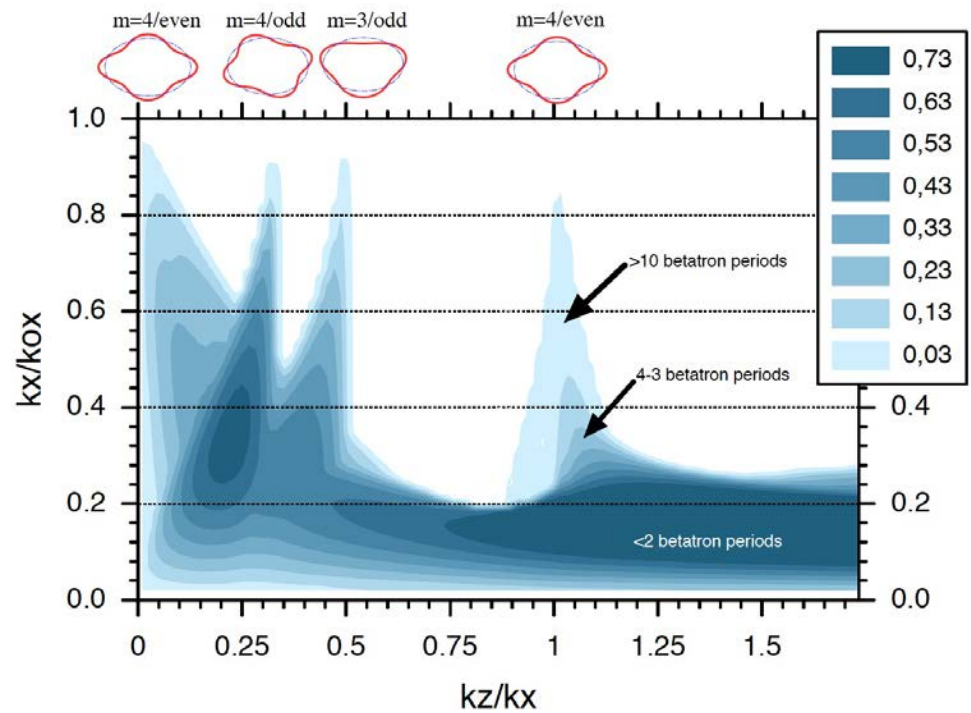
$$\nabla^2 \Phi = -\frac{q}{\epsilon_0} n_1 = -\frac{q}{\epsilon_0} \int f_1 dp_x dp_y.$$

95

Instability of Anisotropic KV Beam



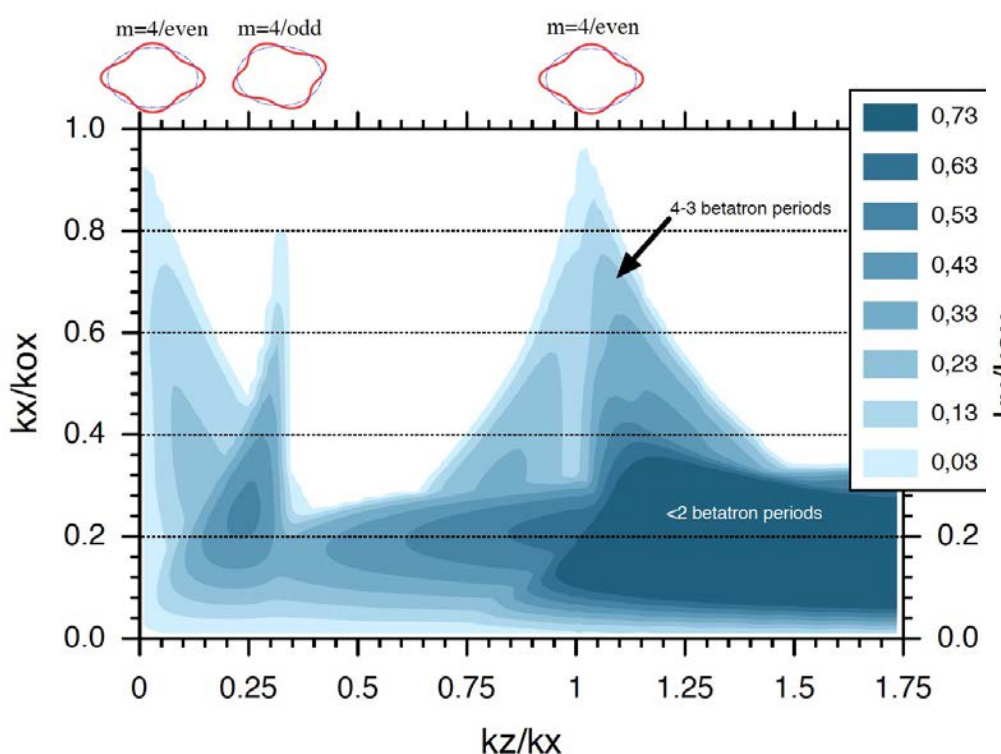
Stability chart for $\epsilon_z/\epsilon_x=0.5$.



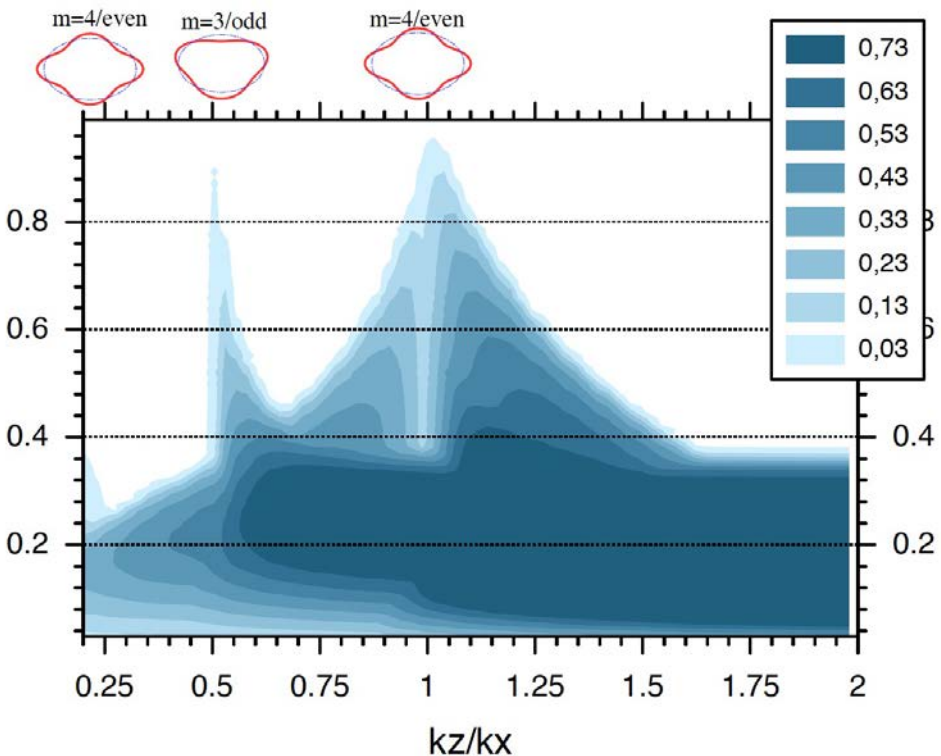
Stability chart for $\epsilon_z/\epsilon_x=1.2$.

Stability charts derived for KV beam with different transverse emittances in focusing channels with different focusing strengths in two transverse directions. Charts are applied to motion in RF field assuming one direction (x-) in transverse and another (z-) is longitudinal.

Instability of Anisotropic KV Beam

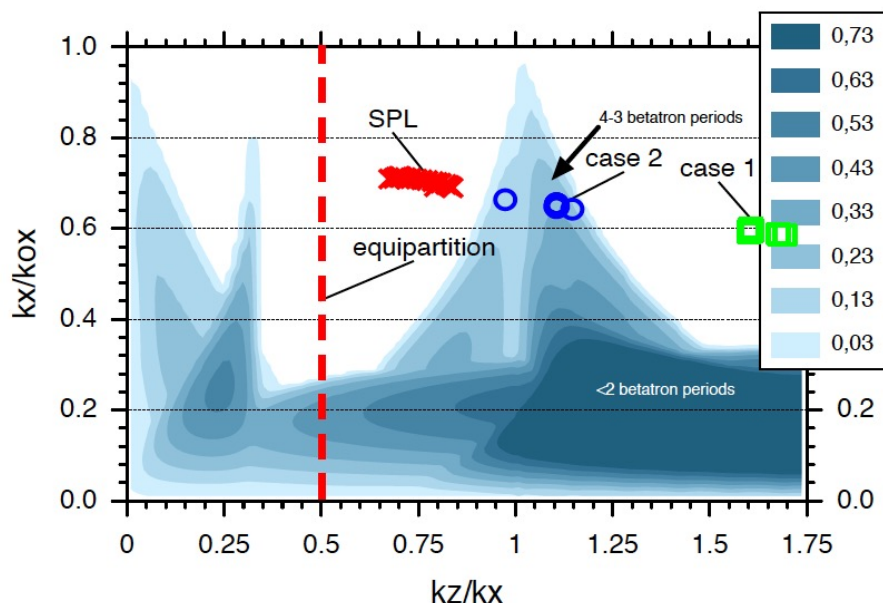


Stability chart for $\epsilon_z/\epsilon_x = 2.0$.

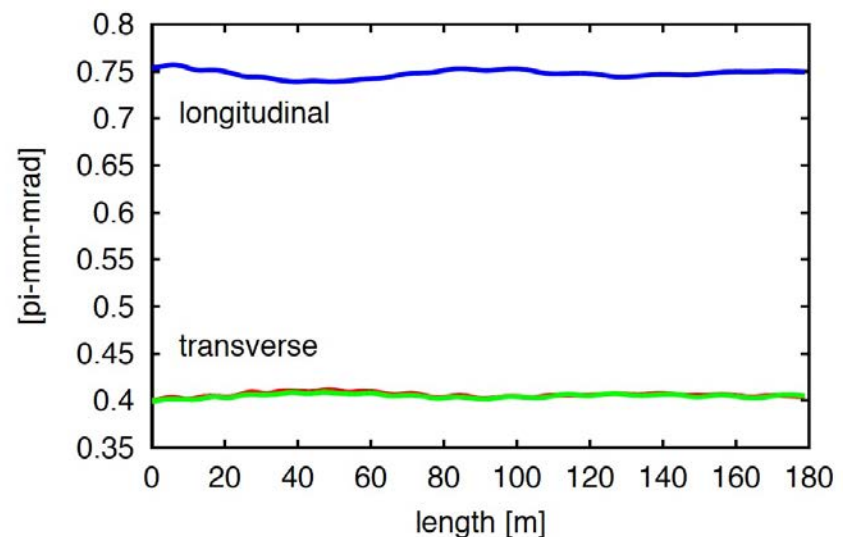


Stability chart for $\epsilon_z/\epsilon_x = 3.0$.

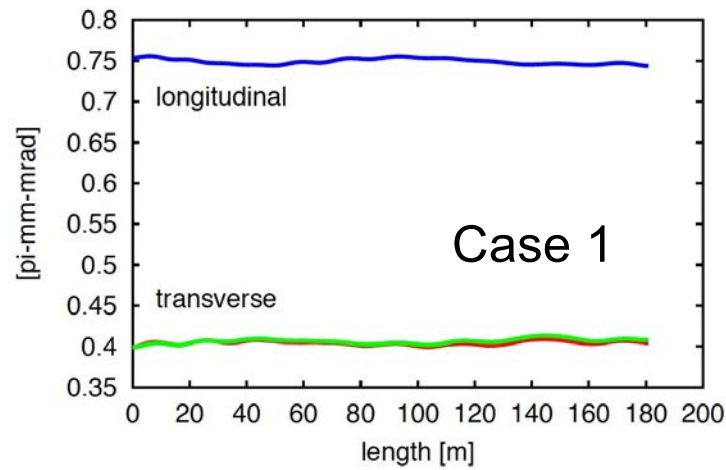
Instability of Anisotropic KV Beam



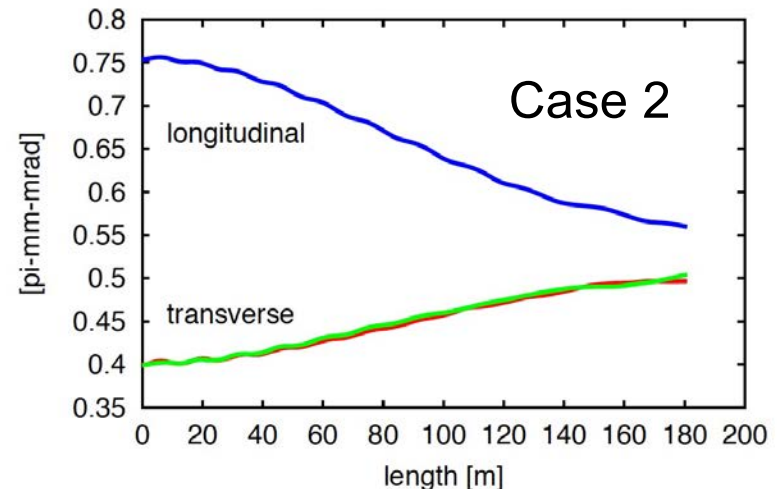
Stability chart for $\epsilon_z/\epsilon_x=2.0$.



Rms emittance evolution for SPL lattice.



Rms emittance evolution



98

Experimental Verification of Stability Charts

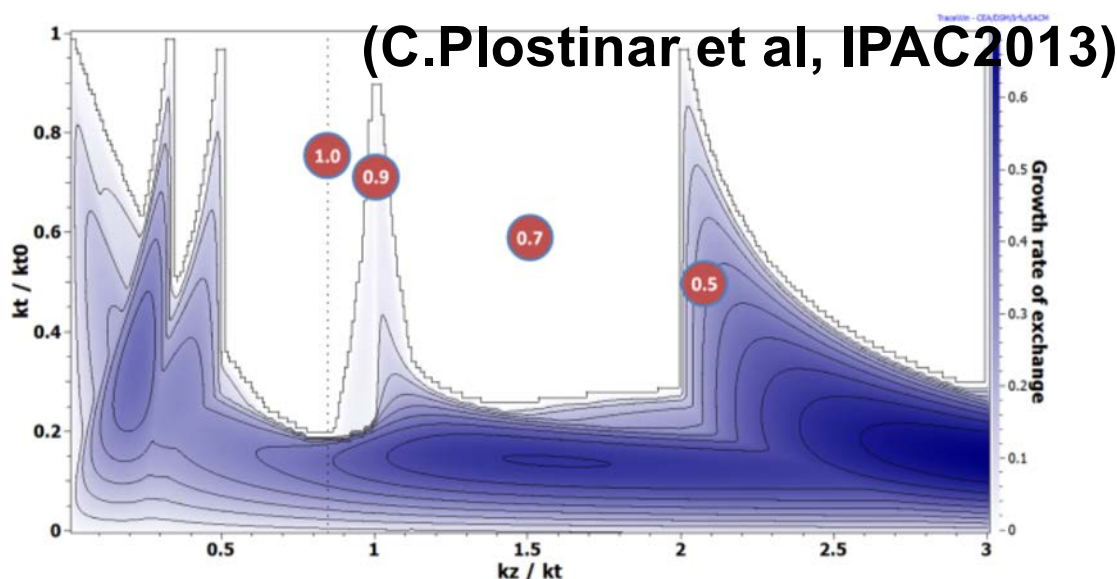


Figure 2: J-PARC linac stability chart for an emittance ratio $\epsilon_z/\epsilon_t = 1.2$. Dotted is the EQP line.

Table 2: Measured emittance values at SDTL15.

T_t/T_z	$\epsilon_t (\pi \cdot \text{mm} \cdot \text{mrad})$	$\epsilon_z (\pi \cdot \text{mm} \cdot \text{mrad})$
1.0	0.216	0.269
0.9	0.229	0.233
0.7	0.253	0.223
0.5	0.293	0.161

Single-particle parametric resonances:
 $k_z / k_x = 2/3, 1, 2$ (see Section 3, slide 86)

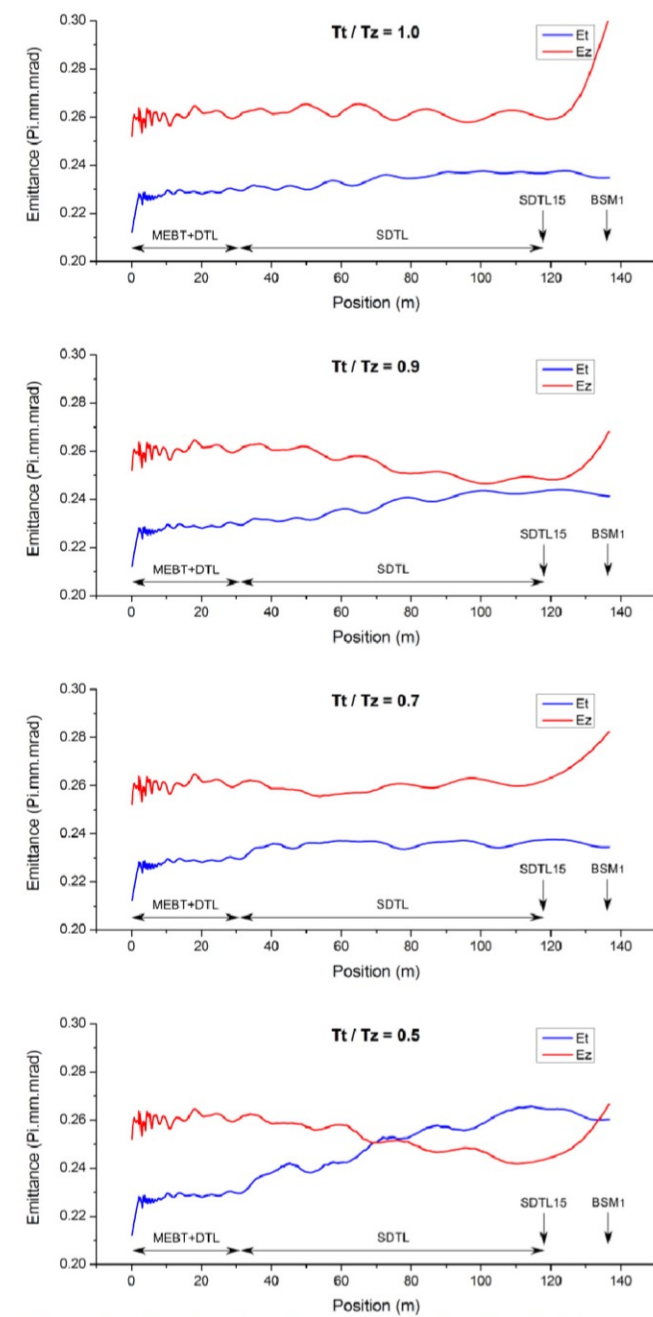
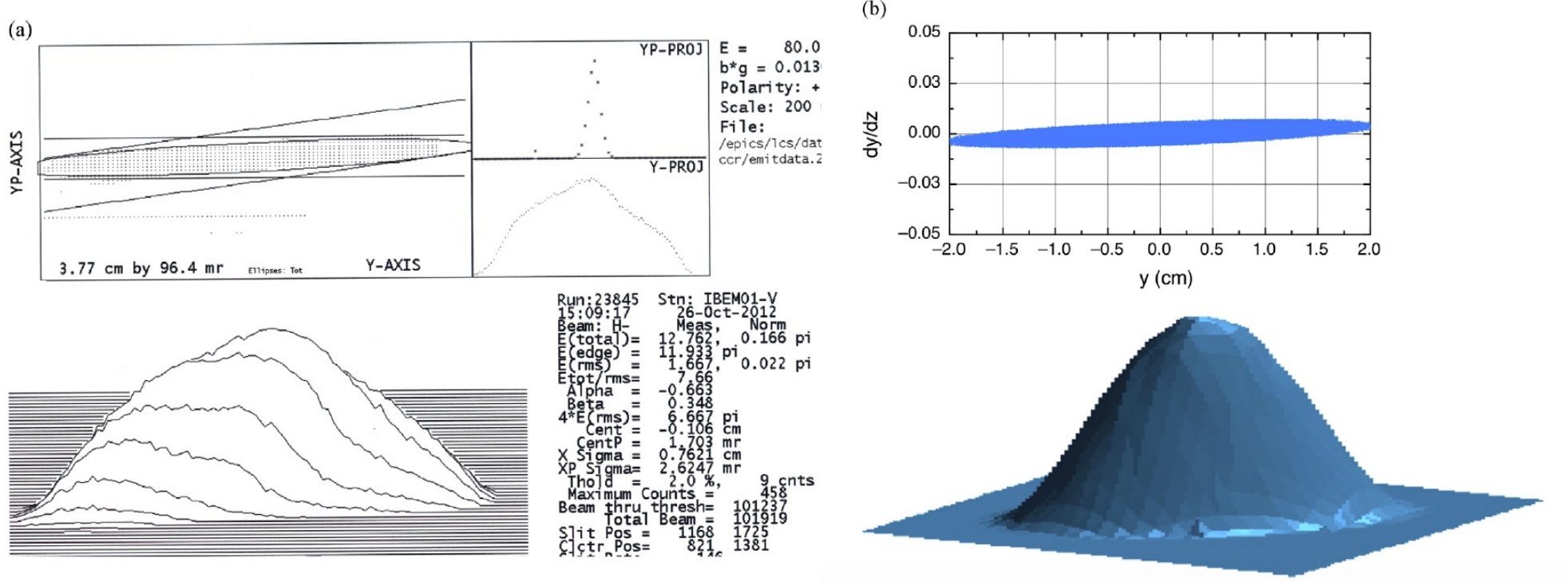


Figure 3: Simulated emittance evolution for the four test cases (RMS Normalised).

Non-Uniform Beam Equilibrium



- (a) Experimentally observed distribution of 80 keV H⁻ beam, extracted from LANL ion source,
- (b) modeling of the same beam with parabolic distribution function in 4D phase space:

$$f = f_o \left(1 - \frac{x^2 + y^2}{2R_b^2} - \frac{p_x^2 + p_y^2}{2p_o^2} \right)$$

100

Non-Uniform Beam Matching in Transport Channel

Beam is matched with continuous (z-independent) focusing channel, if beam distribution function $f(x, p_x, y, p_y)$ is constant.

Self-consistent problem:

Vlasov's Equation

$$\frac{df}{dt} + \frac{\partial f}{\partial \vec{x}} \frac{d\vec{x}}{dt} + \frac{\partial f}{\partial \vec{P}} \frac{d\vec{P}}{dt} = 0$$

Poisson's Equation

$$\Delta U = -\frac{\rho}{\epsilon_0}$$

Solution:

1. Express distribution function as a function of constant of motion (Hamiltonian) $f = f(H)$. Distribution function automatically obeys Vlasov's equation:

$$\frac{df}{dt} = \frac{\partial f}{\partial H} \frac{\partial H}{\partial t} = 0$$

2. Substitute distribution function into Poisson's equation and solve it.

Non-Uniform Beam Matching in Transport Channel (cont.)

Two formulations of the self-consistent beam matching problem:

1. The beam distribution function is known (for example, of the beam extracted from the source). The problem is to find focusing potential, which maintains this distribution in the channel:

$$f(x, p_x, y, p_y) \rightarrow U_{ext}(x, y)$$

2. Potential of the focusing structure is given. The problem is to find the beam distribution function, which is maintained in focusing structure:

$$U_{ext}(x, y) \rightarrow f(x, p_x, y, p_y)$$

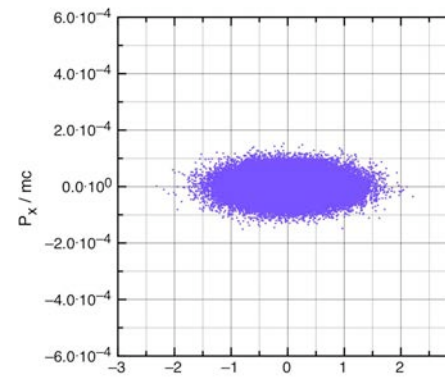
More info:

Y.B. Phys. Rev. E Vol. 53, No. 5, 5358, 1996;
Y.B. Phys. Rev. E Vol. 57, No. 5, 6020, 1998

Equilibrium of a Gaussian Beam

Beam with Gaussian distribution function

$$f = f_0 \exp\left(-2 \frac{x^2 + y^2}{R^2} - 2 \frac{p_x^2 + p_y^2}{p_0^2}\right)$$



Time-independent Vlasov's equation

$$\frac{mc^2}{q} \frac{1}{\gamma} (x p_x + y p_y) = \frac{R^4}{\epsilon^2} \left(p_x \frac{\partial U}{\partial x} + p_y \frac{\partial U}{\partial y} \right)$$

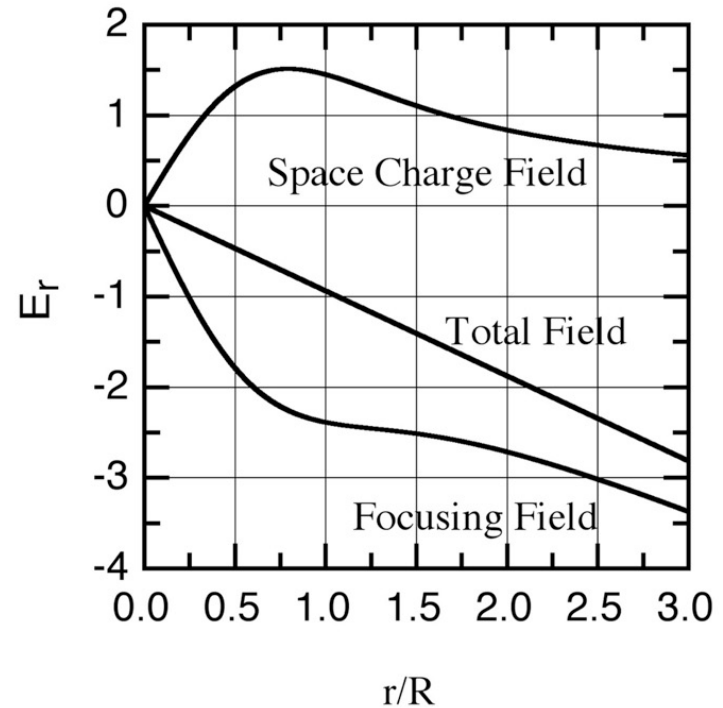
Total potential $U(x,y) = \frac{mc^2}{q} \frac{1}{\gamma} \frac{\epsilon^2}{R^4} \left(\frac{x^2 + y^2}{2} \right)$

Total field $E_{tot} = -\frac{mc^2}{q} \frac{1}{\gamma} \frac{\epsilon^2}{R^4} r$

Space-charge field $E_b = -\frac{\partial U_b}{\partial r} = -\frac{I}{2\pi \epsilon_0 \beta c} \frac{1}{r} \left[1 - \exp\left(-2 \frac{r^2}{R^2}\right) \right]$

Required focusing field

$$E_{ext} = -\frac{mc^2}{q R \gamma} \left[\frac{\epsilon^2 r}{R^3} + 2 \frac{I}{I_c \beta \gamma} \frac{R}{r} \left(1 - \exp\left(-2 \frac{r^2}{R^2}\right) \right) \right]$$



On Equilibrium of a Gaussian Beam

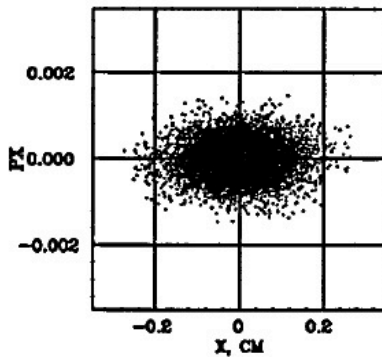
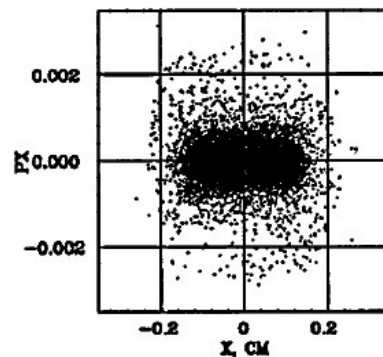
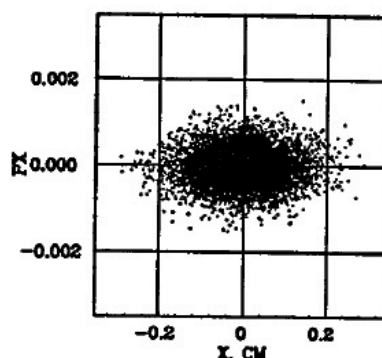
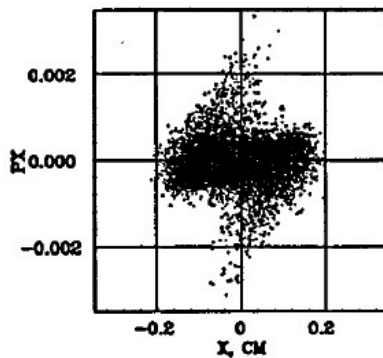
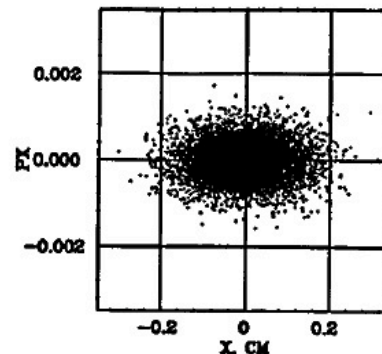
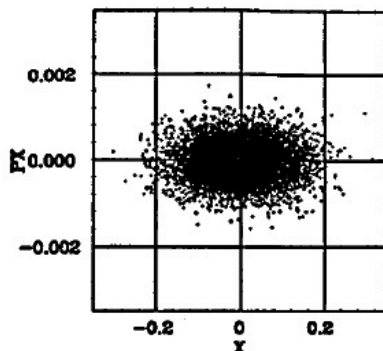


FIG. 7. Mismatching of the Gaussian beam in the linear focusing channel (left column) and matching of the same beam with the nonlinear focusing channel (right column).

Equilibrium of the Beam with “Water Bag” and Parabolic Distributions

WB distribution in phase space

$$f=f_0, \quad \frac{2}{3} \left(\frac{x^2+y^2}{R^2} + \frac{p_x^2+p_y^2}{p_0^2} \right) \leq 1,$$

$$f=0, \quad \frac{2}{3} \left(\frac{x^2+y^2}{R^2} + \frac{p_x^2+p_y^2}{p_0^2} \right) > 1.$$

Parabolic distribution in phase space

$$f=f_0 \left(1 - \frac{x^2+y^2}{2R^2} - \frac{p_x^2+p_y^2}{2p_0^2} \right)$$

Space charge density

$$\rho(r) = \frac{4I}{3\pi\beta c R^2} \left(1 - \frac{2r^2}{3R^2} \right)$$

Space charge density

$$\rho_b = \frac{3I}{2\pi c \beta R^2} \left(1 - \frac{r^2}{2R^2} \right)^2$$

Equilibrium of the Beam with “Water Bag” and Parabolic Distributions

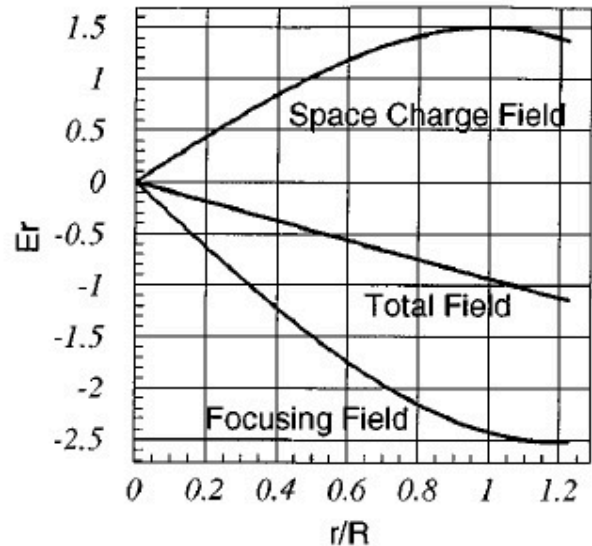


FIG. 4. Total field of the structure E_{tot} [Eq. (12)], required external focusing field E_{ext} [Eq. (21)] and space-charge field E_b [Eq. (20)] of the beam with “water bag” distribution.

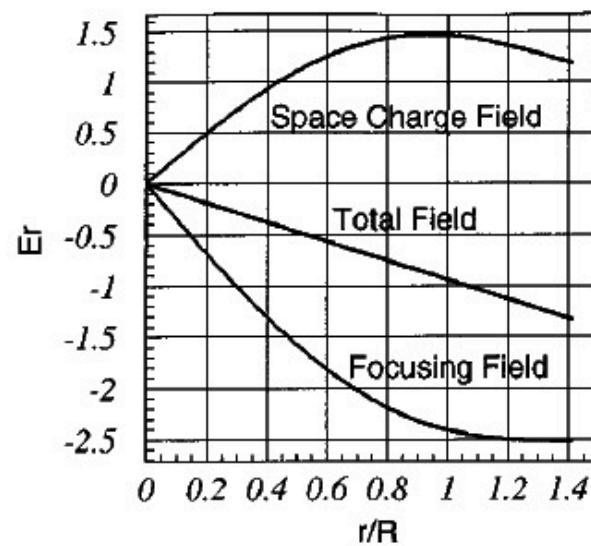
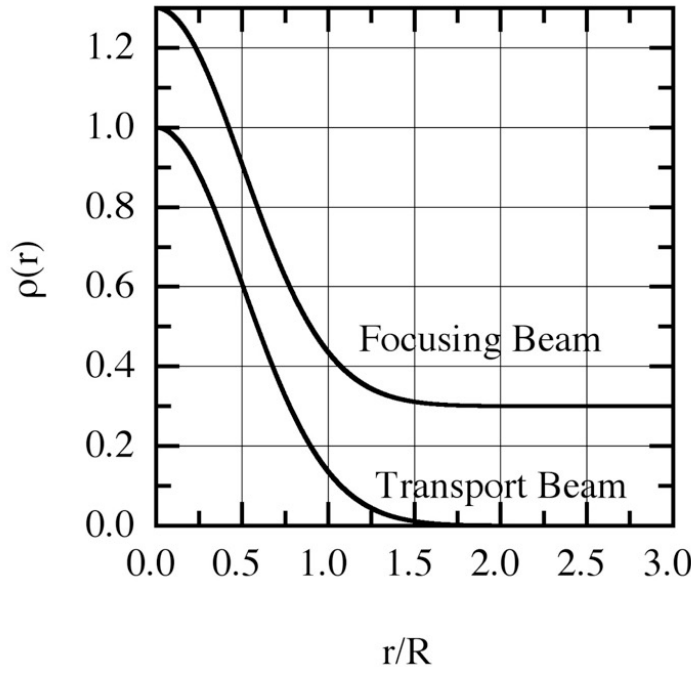


FIG. 5. Total field of the structure E_{tot} [Eq. (12)], required external focusing field E_{ext} [Eq. (25)] and space-charge field E_b [Eq. (24)] of the beam with parabolic distribution.

Focusing by Opposite Charged Particles (Plasma Lens)

Required potential distribution can be created by introducing inside the transport channel an opposite charged cloud of particles (plasma lens) with the space charge density:

$$\rho_{ext} = \rho_0 \exp(-2 \frac{r^2}{R^2}) + \frac{I_c \epsilon^2}{2\pi c R^4}$$



Charged particle density of the transported beam with Gaussian distribution, and of the external focusing beam

Quadrupole-Duodecapole Focusing Structure

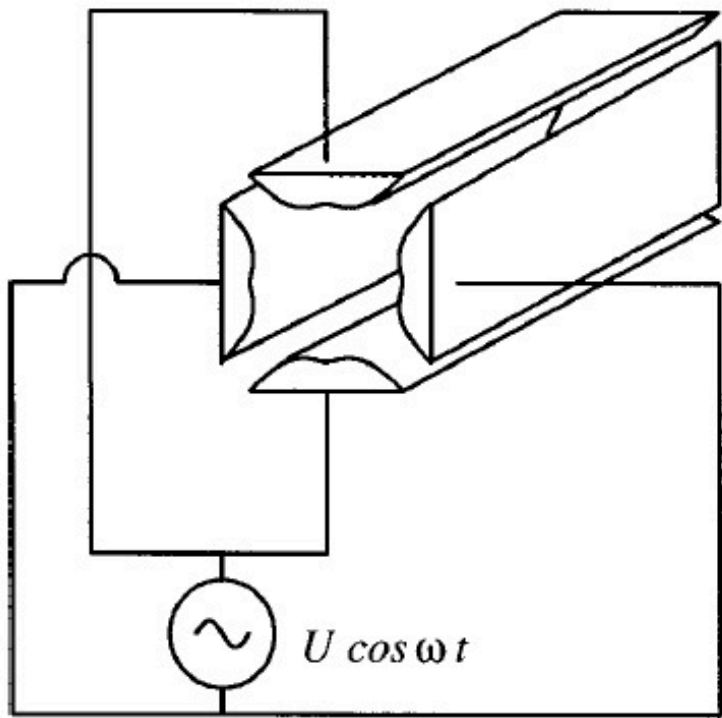


FIG. 6. Proposed four vane quadrupole structure with a duodecapole field component [5].

Potential of the uniform four vanes structure:

$$U(r, \varphi, t) = \left(\frac{G_2}{2} r^2 \cos 2\varphi + \frac{G_6}{6} r^6 \cos 6\varphi \right) \sin \omega_0 t,$$

The electrical field of the structure is given by

$$\vec{E}(r, \varphi, t) = [-\vec{i}_r (G_2 r \cos 2\varphi + G_6 r^5 \cos 6\varphi) + \vec{i}_\varphi (G_2 r \sin 2\varphi + G_6 r^5 \sin 6\varphi)] \sin \omega_0 t.$$

108

Effective Potential of Quadrupole-Duodecapole Focusing Structure

an effective scalar potential of the structure [6]

$$U_{\text{ext}}(\vec{r}) = \frac{q}{4m\gamma} \frac{E_0^2(\vec{r})}{\omega_0^2}, \quad (6.3)$$

which describes the averaged motion of particle. For the considered structure, the effective potential is

$$U_{\text{ext}}(r, \varphi) = \frac{mc^2}{q} \frac{\mu_0^2}{\lambda^2} \left[\frac{1}{2} r^2 + \zeta r^6 \cos 4\varphi + \frac{\zeta^2}{2} r^{10} \right], \quad (6.4)$$

where μ_0 is a smooth transverse oscillation frequency and ζ is a ratio of field components:

$$\mu_0 = \frac{qG_2\lambda^2}{\sqrt{8\pi mc^2}\sqrt{\gamma}}, \quad \zeta = \frac{G_6}{G_2}. \quad (6.5)$$

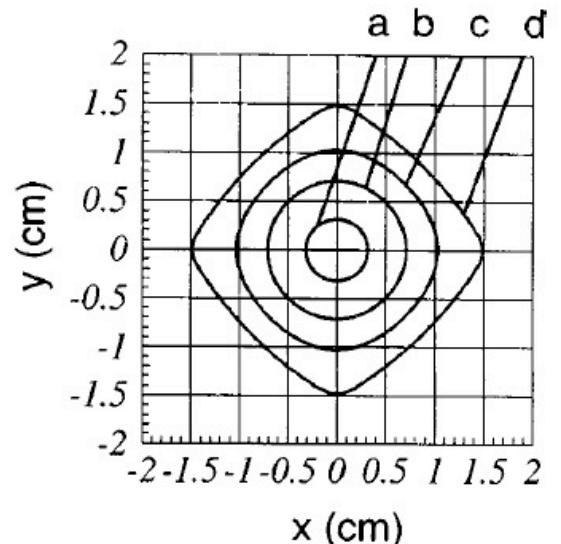


FIG. 7. Lines of equal values of the function $C = \frac{1}{2}r^2 + \zeta r^6 \cos 4\varphi + (\zeta^2/2)r^{10}$ for $\zeta = -0.03$: (a) $C = 0.05$, (b) $C = 0.25$, (c) $C = 0.5$, and (d) $C = 0.85$.

Space-Charge Density of the Matched Beam

The space charge distribution of a matched beam can be derived from Poisson's equation via a known space charge potential of the beam

$$\rho_b = -\epsilon_0 \Delta U_b = \frac{\epsilon_0}{1 + \delta} \gamma^2 \Delta U_{\text{ext}}. \quad (4.26)$$

Application of Eq. (4.26) gives an expression for the self-consistent space charge distribution of the beam in the structure:

$$\rho_b = \rho_0 (1 + 10\zeta r^4 \cos 4\varphi + 25\zeta^2 r^8), \quad (6.6)$$

$$\rho_0 = \frac{2\gamma^2}{(1 + \delta)} \frac{mc^2}{q} \frac{\epsilon_0 \mu_0^2}{\lambda^2}. \quad (6.7)$$

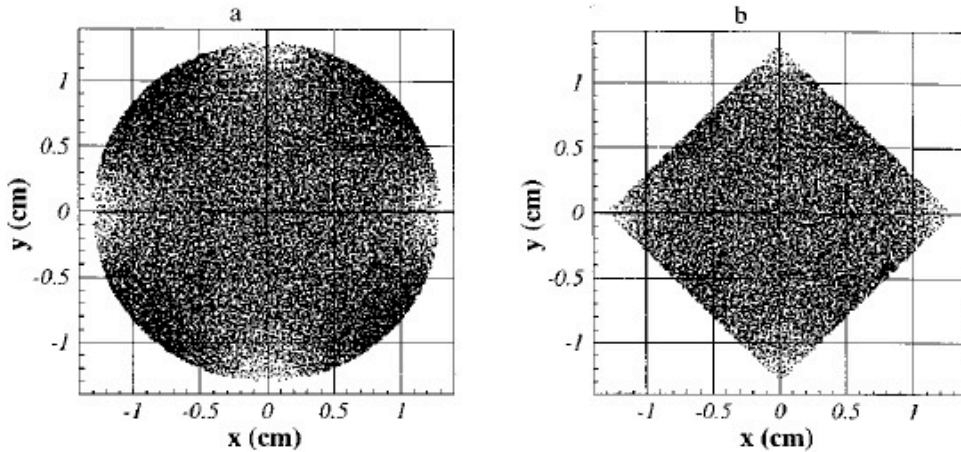


FIG. 8. Self-consistent particle distribution $\rho_b = \rho_0(1 + 10\zeta r^4 \cos 4\varphi + 25\zeta^2 r^8)$ of the matched beam in a quadrupole channel with a duodecapole component with parameter $\zeta = -0.03$: (a) without truncation, (b) with truncation.

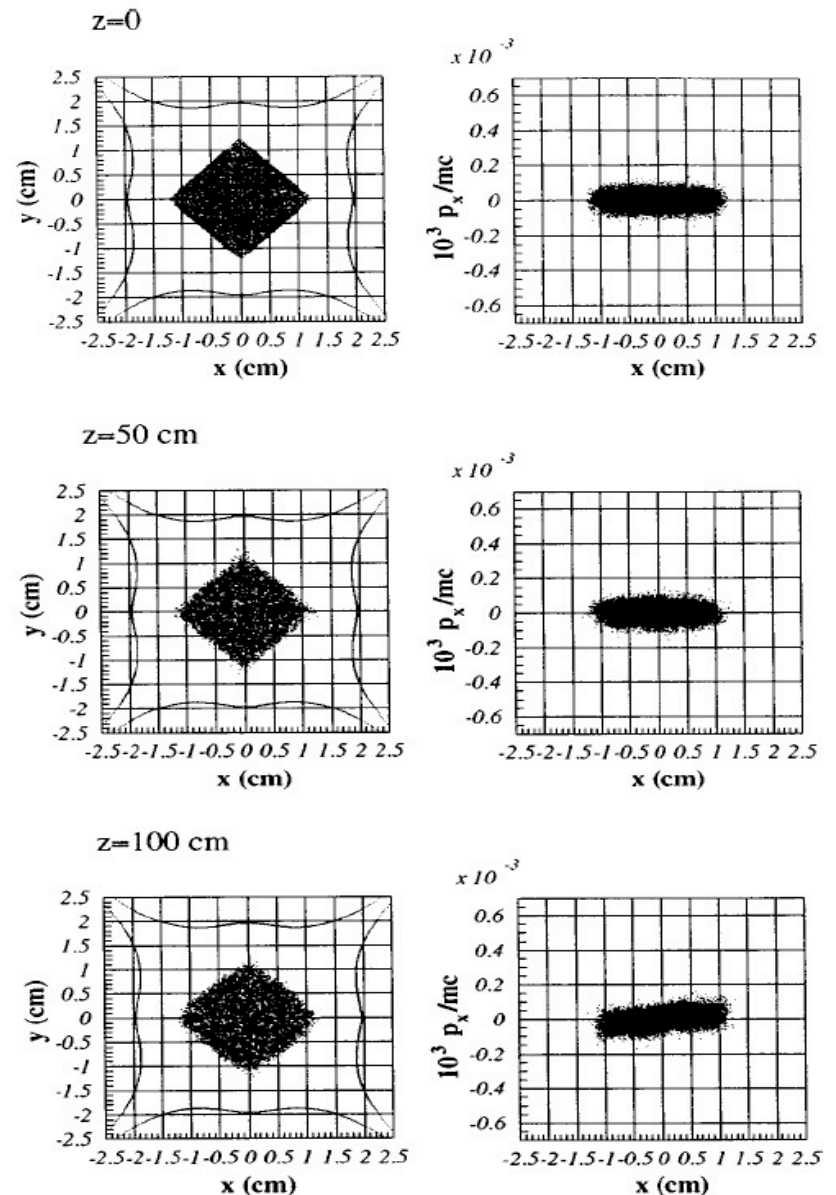
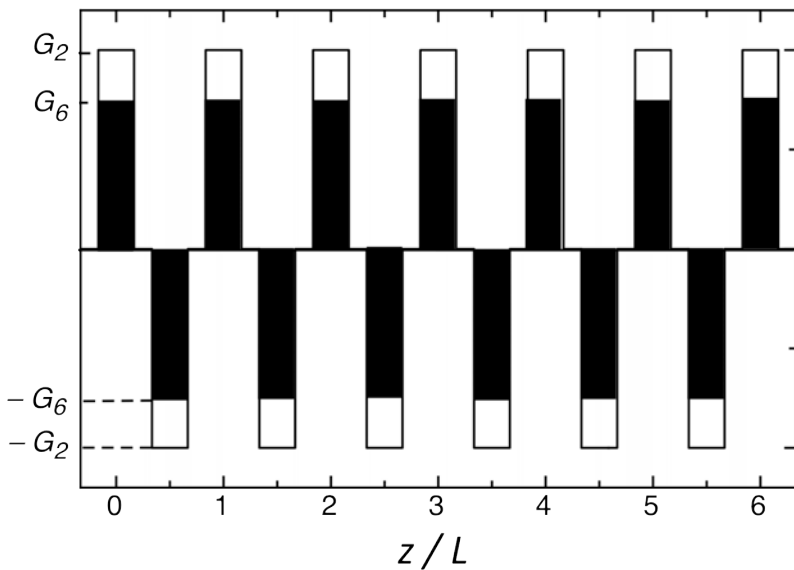


FIG. 9. Emittance conservation of the 150 keV, 100 mA, $0.06\pi \text{ cm mrad}$ proton beam with a matched distribution function (6.14) in a four vane quadrupole structure with field gradient $G_2 = 48 \text{ kV/cm}^2$ and duodecapole component $G_6 = -1.3 \text{ kV/cm}^6$.

FODO Quadrupole - Duodecapole Channel for Suppression of Halo Formation

Effective potential of quadrupole-duodecapole structure:

$$U_{eff} = \left(\frac{\mu_o \beta c}{L}\right)^2 \left[\frac{r^2}{2} + \zeta r^6 \cos 4\theta + \zeta^2 \frac{r^{10}}{2} \right]$$



FODO channel with combined quadrupole $G_2(z)$ and duodecapole $G_6(z)$ field components

Ratio of field components $\zeta = \frac{G_6}{G_2}$

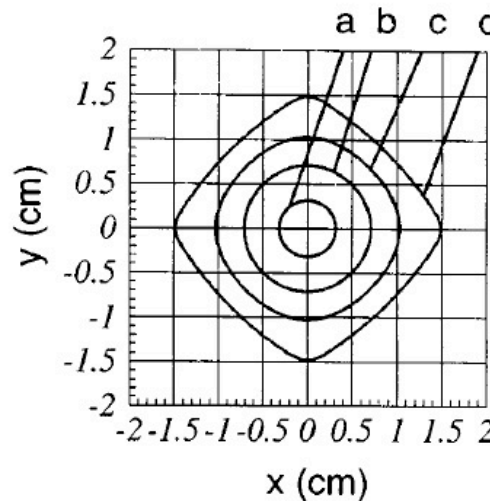
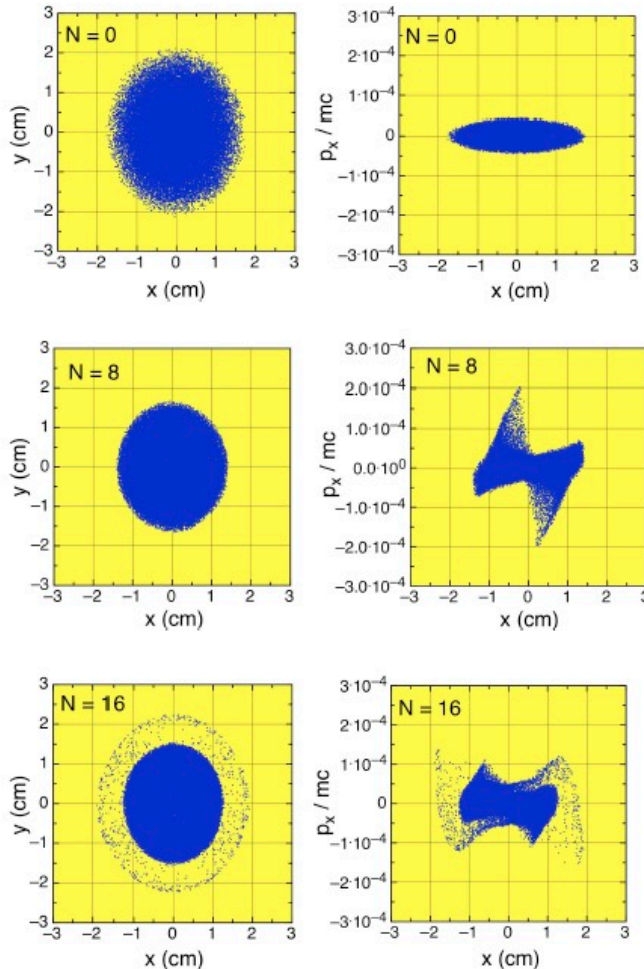


FIG. 7. Lines of equal values of the function $C = \frac{1}{2}r^2 + \zeta r^6 \cos 4\varphi + (\zeta^2/2)r^{10}$ for $\zeta = -0.03$: (a) $C = 0.05$, (b) $C = 0.25$, (c) $C = 0.5$, and (d) $C = 0.85$.

(Y.B. et al NIM-A 816, 2016, p.78–86)

FODO Quadrupole - Duodecapole Channel for Suppression of Halo Formation

Quadrupole Channel



Beam energy

35 keV

Beam current

11.7 mA

Beam emittance

0.05 cm mrad

FODO period

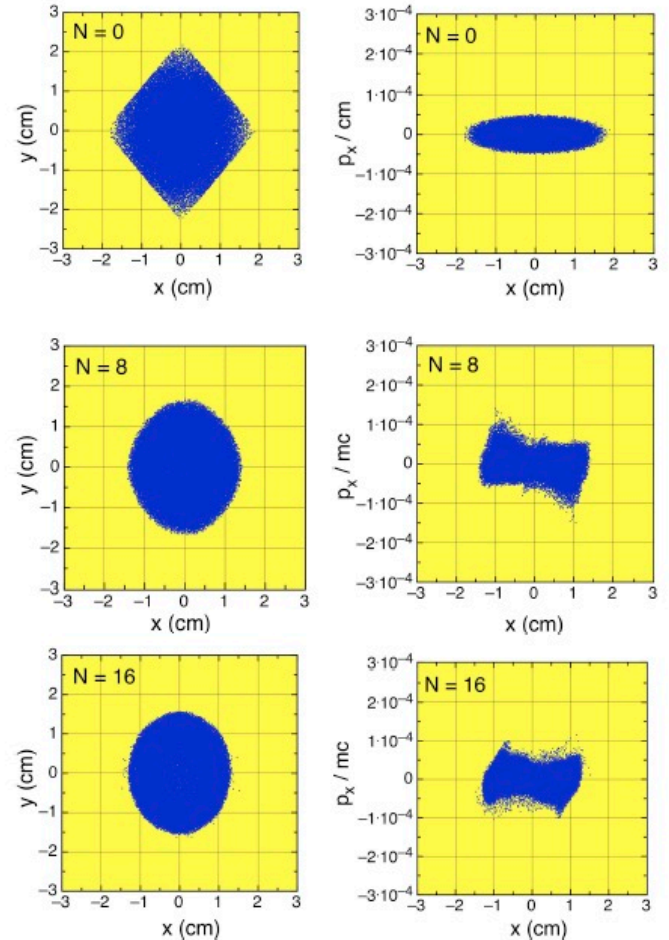
15 cm

Lens length

5 cm

Quadrupole field gradient 0.03579 T/cm

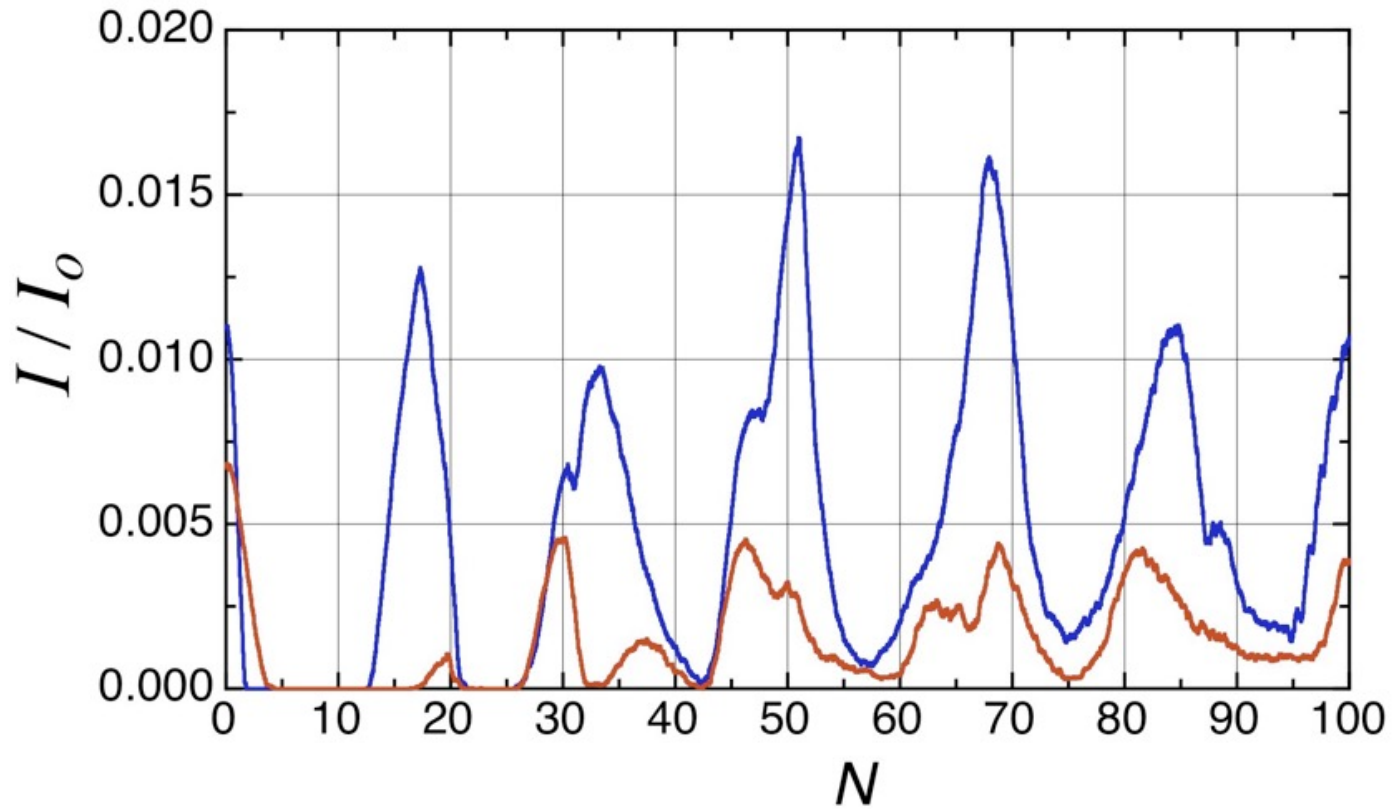
Quadrupole-Duodecapole Channel



Quadrupole field gradient 0.03579 T/cm

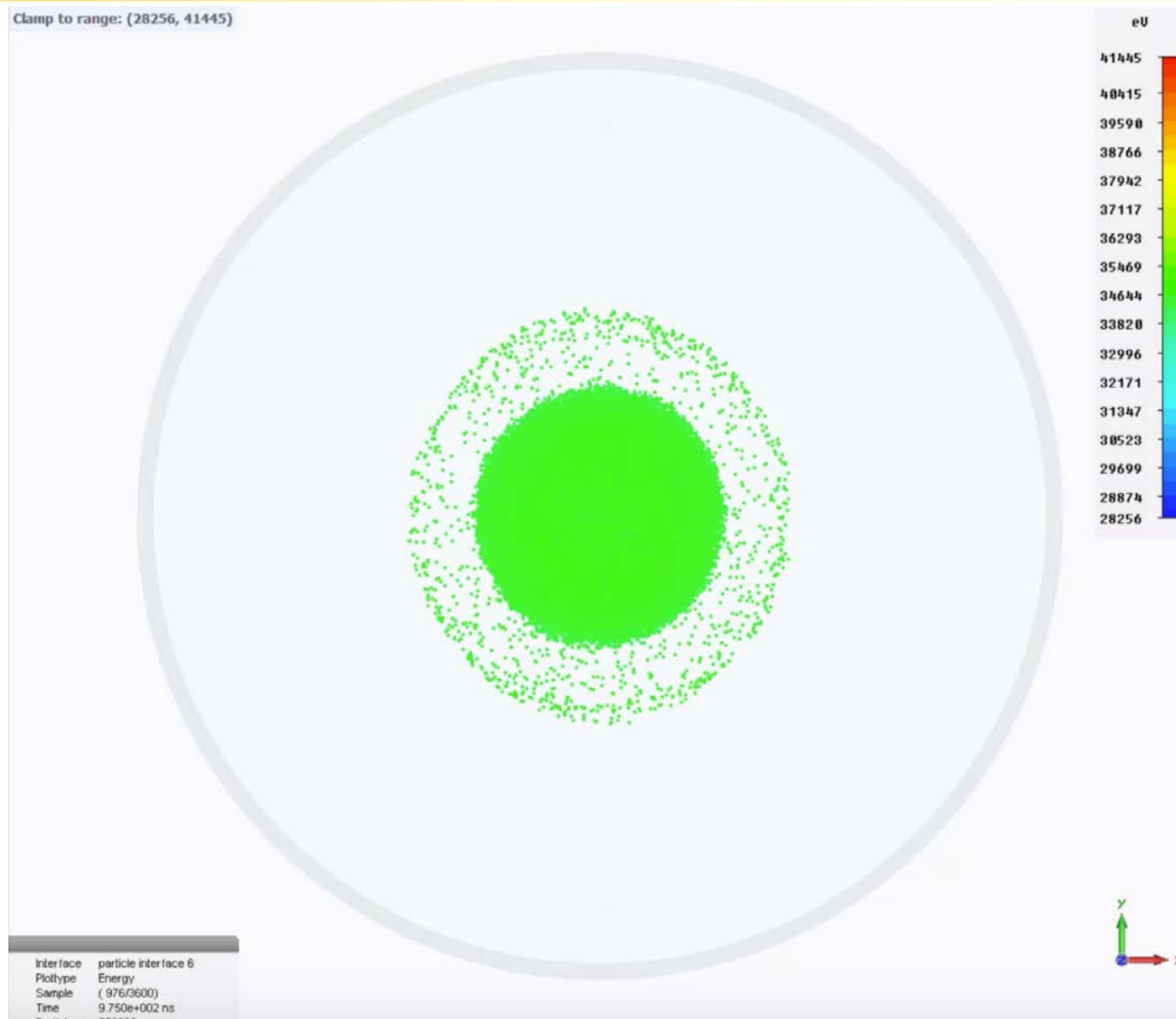
Duodecapole component $G_6 = -1.76e-04 \text{ T/cm}^5$
adiabatically decline to zero at the distance of 7 periods. Numbers indicate FODO periods.

Suppression of Space Charge Induced Beam Halo Formation



Fraction of particles outside the beam core
 $2.5\sqrt{\langle x^2 \rangle} \times 2.5\sqrt{\langle y^2 \rangle}$ as a function of FODO periods: (blue) quadrupole channel, (red) quadrupole-duodecapole channel.

Particle Studio Simulation of Halo Formation in Quadrupole Channel



114

Particle Studio Simulation of Halo Suppression in Quadrupole-Duodecapole Channel

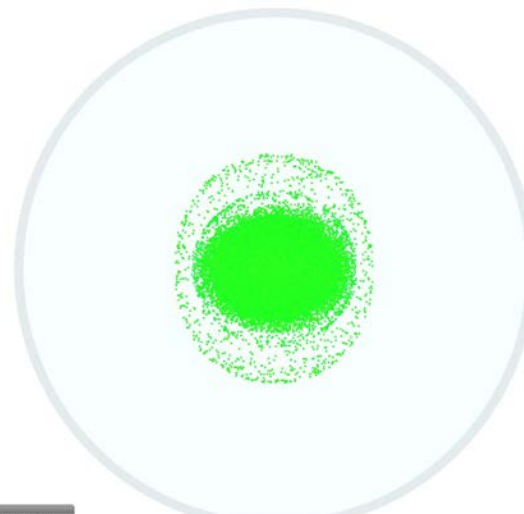


115

Final Particle Distributions in Focusing Channels

Quadrupole Channel

Clamp to range: (28256, 41445)



eV
41445
40815
39598
38766
37942
37117
36293
35469
34644
33828
32998
32171
31347
30523
29699
28876
28056

Plane: particle interface 5
Plottype: Energy
Sample: (1650/3600)
Time: 9.240e-002 ns
Particles: 550000

x
y
z

Plottype: Energy
Sample: (921/1125)
Time: 9.240e-002 ns
Particles: 550000

x
y
z

Clamp to range: (28977, 40550)



eV
40753
39818
39869
38321
37572
36824
36075
35327
34578
33838
33081
32333
31584
30888
29339
28778

x
y
z

Quadruple-Duodecapole Channel

Clamp to range: (28448, 41240)



eV
41240
40621
39441
38847
37842
37083
36262
35444
34644
33895
33195
32396
31596
30867
29987
29168
28448

Los Alamos
NATIONAL LABORATORY

Plane: particle interface 5
Plottype: Energy
Sample: (1650/3600)
Time: 9.240e-002 ns
Particles: 514118

x
y
z

Plottype: Energy
Sample: (920/1125)
Time: 9.240e-002 ns
Particles: 514118

x
y
z

Y. Batygin - USPAS 2021

116

x
y
z